

INTERACTION NOTES

NOTE 522

OCTOBER 1996

COUPLING OF THE HEMP ENVIRONMENT  
TO ABOVE-GROUND WIRES

K.-D. Leuthäuser

Fraunhofer-Institut für Naturwissenschaftlich-Technische Trendanalysen  
P.O. Box 14 91, 53864 Euskirchen, Germany

CLEARED FOR PUBLIC RELEASE

2 Oct 1996

ABSTRACT

The paper deals with the interaction of the electromagnetic pulse environment generated by high altitude bursts (HEMP) with transmission lines. The environment is determined from the TULIP computer code (Theoretical Notes Nos. 363 to 365). The coupling of these fields to above ground conductors is then obtained by time-domain transmission line theory (TLT) assuming a perfectly conducting earth. In particular, the contributions of the vertical potential differences at the end of semi-infinite horizontal lines and different types of vertical line elements (vertical risers) are also discussed within the framework of the TLT rules. The paper presents open-circuit voltages induced in transmission lines at distinct locations within the illuminated area as well as contour plots of peak voltages and cumulative voltage distribution variations.

Fraunhofer Institut  
Naturwissenschaftlich-  
Technische Trendanalysen

Institutsleitung  
Dr. rer. nat. habil. K.-D. Leuthäuser

Appelsgarten 2  
D-53879 Euskirchen

Telefon +49 (0) 22 51/18-1  
Telefax +49 (0) 22 51/182 77

Dr. K.-D. Leuthäuser  
Durchwahl +49 (0) 22 51/18-216  
Telefax +49 (0) 22 51/1 82 77  
e-mail: lth@int.fhg.de

Euskirchen,  
2. Oktober 1996

IN 522

*[Faint, illegible text]*

*[Faint, illegible text]*  
Laboratory (PL / WSR)  
1200 Washington Ave SE

*[Faint, illegible text]*  
Tel: +1 877-117-5776

Dear Dr. Baum

I enclose 2 mastercopies of a paper "Coupling of the HEMP Environment to  
Above Ground Wires".

I would appreciate to have the paper published in the Interaction Notes series.

Sincerely

*[Handwritten signature]*  
K.-D. Leuthäuser

Vorstand der Fraunhofer-Gesellschaft:  
Prof. Dr.-Ing. Dr. h. c. mult.  
Hans-Jürgen Warnecke, Präsident  
Dr. jur. Dirk-Meints Polter  
Dr. rer. pol. Hans-Ulrich Wiese

Fraunhofer-Gesellschaft zur Förderung  
der angewandten Forschung e. V., München

Bankverbindung: Deutsche Bank, München  
Konto 7521933 RI 7 700 700 10



DEPARTMENT OF THE AIR FORCE  
PHILLIPS LABORATORY (AFMC)

Date: 22 NOV 96

MEMORANDUM FOR PL/WSQW

ATTENTION: Dr. Carl E. Baum

FROM: PL/PA

SUBJECT: Phillips Laboratory Security Review Case Number(s) PL 96-1179

1. Action on the security review case mentioned above has been completed with the following determination, as marked:

**CLEARED FOR OPEN PUBLICATION/PRESENTATION (NO CHANGES.)**

**CLEARED FOR OPEN PUBLICATION/PRESENTATION AS AMENDED.** The amendments, changes, deletions, etc., denoted by the words "as amended? -- are mandatory. Words of information to be deleted are indicated inside brackets.

**CLEARED FOR OPEN PUBLICATION/PRESENTATION WITH RECOMMENDED CHANGES.** The reviewers have suggested some changes which are not mandatory, indicated by the words "recommended changes."

**DISAPPROVED FOR PUBLIC RELEASE** for the following reason(s)

Contained Classified Information

Contained Technology Security Information Determined Not to be releasable to the public

Release Denied for other AF/DoD/Government reasons

The PL project officer must notify the author/contractor about the decision on this case and send them a copy of this letter with a copy of the stamped document (attached).

**OTHER:** \_\_\_\_\_

If you have questions, please call me at (505) 846-6246.

  
JUDY L. JOHNSTON  
Security Review Officer

Attachments:

PL 96-1179

INTERACTION NOTES

NOTE 522

OCTOBER 1996

**COUPLING OF THE HEMP ENVIRONMENT  
TO ABOVE-GROUND WIRES**

K.-D. Leuthäuser

Fraunhofer-Institut für Naturwissenschaftlich-Technische Trendanalysen  
P.O. Box 14 91, 53864 Euskirchen, Germany

ABSTRACT

This paper deals with the interaction of the electromagnetic pulse environment generated by high altitude bursts (HEMP) with transmission lines. The environment is determined from the EXEMP computer code (Theoretical Notes Nos. 363 to 365). The coupling of these fields to above-ground conductors is then obtained by time-domain transmission line theory (TLT) assuming a perfectly conducting earth. In particular, the contributions of the vertical potential differences at the end of semi-infinite horizontal lines and different types of vertical line elements (vertical risers) are also discussed within the framework of the TLT rules. The paper presents open-circuit voltages induced in transmission lines at distinct locations within the illuminated area as well as contour plots of peak voltages and cumulative voltage distribution functions.


## 1. Introduction

The interaction of ground-based electric systems with an incident electromagnetic pulse generated by a high-altitude nuclear event (HEMP) is commonly investigated using worst case standard waveforms [1, 2] artificially combining the highest peak electric fields with the shortest rise-times and the largest time integrals of all possible waveforms which can be encountered on the earth's surface. It is in the nature of such pulses that they overestimate the coupling to systems. In order to avoid overprotection of a hardened system, e.g. because of economic constraints, a more detailed analysis considering the distribution of the targets within the HEMP illuminated region and also lower nuclear yields seems to be desirable.

The purpose of the present paper is to combine the whole variety of HEMP manifestations (i.e. by variation of the system location with respect to Ground Zero) and the interaction of the incident field with the system. This approach was already followed by F.M. Tesche [3-5] who studied the excitation of transmission lines by a more realistic HEMP environment than worst case. There are several reasons for an independent reevaluation of these former results:

- Test of compatibility of CHAP code [6] and EXEMP code [7-9] results for the HEMP environment
- Consideration of nuclear gamma yields less than 10 kt (as assumed by CHAP code)
- Variation of transmission line heights above ground
- More detailed treatment of different vertical elements ("risers") than by means of a single approximate expression.


Open-circuit voltage contributions of vertical line elements may even dominate the contribution of horizontal conductors in a transmission line system. For example, the currents and voltages induced in a horizontal line can become negligibly small when approaching the tangent radius (i.e. the horizon of the illuminated area), while for a vertical element open-circuit voltages of up to several hundred kilovolts can be obtained. This is particularly the case when assuming a perfectly conducting ground where the horizontal components of the incident and reflected electric field (i.e. a horizontally polarized wave as well as the horizontal electric field component of a vertically polarized wave) annihilate (reflection coefficient  $R = -1$ ), and add for the vertical component (i.e. the vertical component of the electric field of a vertically polarized wave) for which  $R = +1$ . Hence, the assumption of a perfectly conducting ground generally underestimates the EMP coupling to horizontal lines and overestimates the effects on vertical elements. Because the present paper is focused on the interaction with vertical elements and



upper limits for induced currents and voltages, this assumption seems to be justified. Furthermore, it has the advantage of admitting analytical time domain solutions within the framework of transmission line theory.

After this introduction, Section 2 reviews the basic features of the EXEMP code, required input data and some numerical results of the free field environment.


Section 3 reviews time domain transmission line solutions to semi-infinite lossless lines without vertical elements. Spatial variations of the EMP fields along the line will not be considered for simplicity. Hence, "semi-infinite" means that the line is not longer than some characteristic length (typically a few kilometers) describing the spatial field variations. Since the duration of the induced pulses never exceeds 1  $\mu$ s, a conductor of the length of some 300 m can already be considered as infinitely long. Therefore, the above condition is always satisfied.



It will be shown how the induced peak voltages vary depending on the position with respect to Ground Zero within the illuminated area. Assuming uniform-area distributions of transmission lines and uniform angular distribution with respect to the propagation vector of the incident electromagnetic wave, cumulative distribution functions and mean values for the induced voltages will be derived.

Also considered are the effects of a less severe threat environment than that considered by other authors [3-6]. To this purpose, environments for heights of burst and gamma yields different from the standard reference environment ( $H_0 = 400$  km,  $Y_\gamma = 10$  kt) [6] were generated by means of the EXEMP code [7].

Section 4 is devoted to the interaction with vertical line elements and their combination with horizontal conductors. Four types of vertical elements are specified according to different terminations at the top and the base, respectively.



Since the incident wave is horizontally polarized along the geomagnetic meridian through GZ (i.e. in northward and southward directions) vertical elements at those positions act only as passive impedances with delay times associated with their length [10]. For locations in eastward or westward directions the contributions of vertical risers can become quite considerable despite their short length. As already mentioned, they may even dominate when approaching the horizon of the illuminated area.

## 2. The EXEMP-HEMP Environment

EXEMP is a self-consistent physics-based code for calculation of the HEMP environment [7-9]. It determines the incident electromagnetic pulse which can be decomposed into horizontally and vertically polarized waves at any observer position within the total area of coverage on a curved earth surface. Standard input data comprise a nuclear gamma yield of 10 kt and a height of burst of 200 km. A QEXP type gamma source function (quotient of the sum of two exponentials) was chosen which is also defined for negative times. The time-constant for the rising part of the gamma pulse was assumed to be  $\alpha = 2.0/\text{ns}$ , the constant for decay was chosen as  $\beta = .1/\text{ns}$ .

The resulting EMP fields are also defined for negative time. The maximum peak electric field magnitude of about 60 kV/m is obtained for an observer position  $1.4 \times \text{HOB} = 280 \text{ km}$  south of Ground Zero. At the tangent radius, the peak electric field drops down to about 26 kV/m. Furthermore, rise-times between 1 and 5 ns and time integrals of the electric field magnitude up to .002 Vs/m are obtained.

*Horizontal polarization dominates throughout the coverage area. Along the meridian though GZ, the wave has practically no vertical contribution (polarization degree  $P_H = 1, P_V = 0$ ). The maximum vertical polarization  $P_V \approx 0.4$  is obtained for observer positions east and west of Ground Zero.*

Because only the vertical component of a vertically polarized wave is responsible for coupling to a vertical transmission line element, the electric fields are also decomposed according to their horizontal and vertical components with respect to the earth surface. The vertical electric field has its maximum of 22 kV/m at about  $2.5 \times \text{HOB}$  east and west of Ground Zero. At the western and eastern horizons, the vertical field strengths still amount to over 10 kV/m.

## 3. Coupling to Semi-Infinite Lines

This section considers the HEMP coupling to semi-infinite horizontal transmission lines over a perfectly conducting ground. Due to this idealization, closed-form analytic solutions can be obtained in time-domain when applying transmission line theory.

As in the literature [7], a coordinate system is introduced such that the z-axis is in the air-ground interface. The conductor is in the direction of the negative z-axis and open at  $z=0$ .  $\phi$

and  $\psi$  are the azimuth and elevation angles of the propagation vector of the incident wave, respectively.

According to transmission line theory, the z-component of an incident electric field induces voltage pulses  $E_z(z) dz/2$  on each element  $dz$  of the conductor traveling with the speed of light in positive and negative z-directions. The sign of the pulse is positive (negative) when propagating in the positive (negative) z-direction. At  $z = 0$ , the pulse is reflected, thus doubling the open-circuit voltage contribution of the line element  $dz$  at  $z$ .

Defining  $t = 0$  as the time where the incident pulse first arrives at the open end  $z = 0$  of the conductor and considering the proper retardation for arrival at line elements  $z < 0$ , the open-circuit voltage at  $z = 0$  developed by a horizontally polarized incident pulse  $E_h(t)$  is

$$V_{oc,h}^{(i)} = \sin \varphi \int_{-\infty}^0 E_h \left( t - \frac{z}{c} \cos \varphi \cos \psi + \frac{z}{c} \right) dz . \quad (1)$$

The corresponding expression for the pulse reflected from the air-ground interface is

$$V_{oc,h}^{(r)} = -\sin \varphi \int_{-\infty}^0 E_h \left( t - \frac{z}{c} \cos \varphi \cos \psi + \frac{z}{c} - \frac{2h}{c} \sin \psi \right) dz \quad (2)$$

with the negative sign because of  $R_h = -1$ .

Assuming that  $\psi$  does not depend on  $z$  (which, due to the earth surface curvature, does not apply near the horizon), the total voltage becomes

$$\begin{aligned} V_{oc,h} &= V_{oc,h}^{(i)} + V_{oc,h}^{(r)} \\ &= \frac{c \sin \varphi}{1 - \cos \varphi \cos \psi} \left( \int_{-\infty}^t E_h(t') dt' - \int_{-\infty}^{t-t_r} E_h(t') dt' \right) \\ &= \frac{c \sin \varphi}{1 - \cos \varphi \cos \psi} \int_{t-t_r}^t E_h(t') dt' \end{aligned} \quad (3)$$

$$\text{where } t_r = \frac{2h}{c} \sin \psi . \quad (4)$$



For a vertically polarized incident wave  $E_v(t)$  only the component  $E_v \sin \psi \cos \varphi$  is effective (i.e. is in direction of the conductor). Because the reflection coefficient is also -1, the open-circuit voltage becomes

$$V_{oc, v} = \frac{c \cos \varphi \sin \psi}{1 - \cos \varphi \cos \psi} \int_{t-t_r}^t E_v(t') dt'. \quad (5)$$

Any arbitrary electric field vector of the incident wave can be decomposed into waves with horizontal and vertical polarization. The total coupling to a horizontal line is therefore given by

$$\begin{aligned} V'_{oc}(t) &= V_{oc, h} + V_{oc, v} \\ &= \frac{c}{1 - \cos \varphi \cos \psi} \left( \sin \varphi \int_{t-t_r}^t E_h(t') dt' + \cos \varphi \sin \psi \int_{t-t_r}^t E_v(t') dt' \right). \end{aligned} \quad (6)$$

For small elevation angles  $\psi$ , Eq. (6) can be approximated by

$$V'_{oc}(t) \approx 2h \frac{\sin \psi}{1 - \cos \varphi \cos \psi} (\sin \varphi E_h(t) + \cos \varphi \sin \psi E_v(t)). \quad (7)$$

However, this approximation is not applicable on or very close to the tangent radius. Even if the semi-infinite line ends on or beyond the horizon, the incident pulse always interacts with line elements within the illuminated area for which  $\psi = \psi(z) > 0$  because of the curvature of the line. Hence, Eq. (1) can no longer be evaluated analytically. It is only for  $\varphi = 90^\circ$  (i.e. the transmission line runs parallel to the horizon) that  $\psi$  does not depend on  $z$  such that (7) yields

$$\lim_{\psi \rightarrow 0} V'_{oc}(t) = 0 \quad \text{for} \quad \varphi = \pi / 2. \quad (8)$$

Eq. (6) describes the open-circuit voltage between the end  $z=0$  of a semi-infinite transmission line and the ground. If there are no vertical line elements reaching from the surface to the horizontal conductor which reduce the open-circuit voltage (6) by interaction with the vertical component of the resultant E-field, Eq. (6) should instead be reduced by the potential difference of the free field between the ground and the horizontal conductor. This potential difference  $V$  is determined as follows for the incident and reflected wave [11]

$$\begin{aligned}
 V(t) &= \cos \psi \int_0^h E_v \left( t - \frac{h-x}{c} \sin \psi \right) dx + \cos \psi \int_0^h E_v \left( t - \frac{h-x}{c} \sin \psi - \frac{2x}{c} \sin \psi \right) dx \\
 &= c \operatorname{ctg} \psi \int_{t-t_r}^t E_v(t') dt'
 \end{aligned} \tag{9}$$

by integration over  $E_x = \cos \psi E_v$  along a fictitious vertical riser of height  $h$  in the direction of the  $x$ -axis. In this case, the reflection coefficient is  $R = +1$  because only the vertical component of the electric field vector is involved. The "effective" open-circuit voltage is then given by

$$V_{oc}(t) = V'_{oc}(t) - V(t). \tag{10}$$

At the horizon, Eq. (9) reduces to

$$\lim_{\psi \rightarrow 0} V(t) = 2h E_v(t). \tag{11}$$

According to Section 2, at the western and eastern horizons the vertical component  $E_x$  of the electric field can reach peak values of 10 kV/m. The maximum potential difference therefore becomes

$$V_{pk} = 2h E_{x, pk} \approx 2 \cdot 10^5 \text{ V/m} \tag{12}$$

for a vertical conductor of height  $h = 10$  m.

The EXEMP calculations exhibit negligible rotation of the electric field vector during the pulse duration. Hence, the time dependence of the different field components is almost identical, and their respective peak values coincide in time. This also applies for the peak values of the integrals in Eqs. (6) and (9). Therefore, the induced voltages peaks correspond to the peaks of the integrals and

$$V_{pk}(\varphi, \psi) = \operatorname{Max}_{\{t\}} V_{oc}(t) = \frac{1}{1 - \cos \varphi \cos \psi} (\sin \varphi I_h + \cos \varphi \sin \psi I_v) - \operatorname{ctg} \psi I_v \tag{13}$$

where

$$I_{h,v} \approx c \operatorname{Max}_{\{t\}} \int_{t-t_r}^t E_{h,v}(t') dt'. \quad (14)$$

For a given position of the conductor with respect to Ground Zero,  $I_h$ ,  $I_v$  and  $\psi$  are determined, but the azimuth angle  $\varphi$  (i.e. to orientation of the transmission line) can still be chosen arbitrarily. For a worst case analysis,  $\varphi$  will be determined such that

$$V_{\max}(\psi) = \operatorname{Max}_{\{\varphi\}} V_{pk}(\varphi, \psi) \equiv V_{pk}(\varphi_{\max}, \psi). \quad (15)$$

From the condition

$$\frac{\partial V_{pk}(\varphi, \psi)}{\partial \varphi} = 0 \quad (16)$$

after a lengthy calculation one arrives at the two azimuth angles

$$\cos \varphi_{\max} = \cos \varphi_{1,2} = \frac{\cos \psi I_h^2 \pm \sin^2 \psi I_v I_{\text{tot}}}{I_{\parallel}^2} \quad (17)$$

$$\text{with } I_{\text{tot}} = \sqrt{I_h^2 + I_v^2} \quad (18)$$

$$I_{\parallel} = \sqrt{I_h^2 + \sin^2 \psi I_v^2} \quad (19)$$

Substituting (17) in (13) yields

$$V_{\max} = \pm \frac{I_{\text{tot}}}{\sin \psi}. \quad (20)$$

If the potential difference (9) had not been considered in (10), the analogous expression would be

$$V'_{\max} = \frac{I_{\text{tot}}}{\sin \psi} \left( \frac{I_x}{I_{\text{tot}}} \pm 1 \right) = \operatorname{ctg} \psi I_v \pm \frac{I_{\text{tot}}}{\sin \psi} \quad (21)$$

In this case, the absolute values of the two maxima are no longer identical. The absolute maximum voltage is given by

$$|V'_{\max}| = \frac{I_{\text{tot}}}{\sin \psi} + \text{ctg} \psi |I_v|. \quad (22)$$

If the polarization is purely horizontal, the condition (12) is satisfied by

$$\varphi_{1,2} = \pm \psi, \quad (23)$$

and

$$V_{\max} = \pm \frac{I_{\text{tot}}}{\sin \psi} = \pm \frac{I_h}{\sin \psi}. \quad (24)$$

For sufficiently small elevation angles  $\psi > 0$ , Eq. (17) becomes

$$\cos \varphi_{1,2} = \cos \psi - \varepsilon^2 \sin^2 \psi \left( 1 \pm \sqrt{1 + 1/\varepsilon^2} \right) + O(\sin^4 \psi) \quad (25)$$

where  $\varepsilon = I_v / I_h \approx E_v / E_h$ .

Hence, the angular separation of the minimum and the maximum is of second order in  $\sin \psi$ . Nevertheless, it remains finite at the horizon because of the  $z$  dependence of  $\psi$  along the transmission line.

## Numerical Results

The numerical results comprise two sets of diagrams, the first of which (Figures 1 to 10) shows induced open-circuit voltages as a function of time for various azimuth angles  $\varphi$  at distinct positions within the illuminated area, the second set (Figures 11 to 21) deals with the variation of peak voltages with the position and integral data, such as mean voltages when averaged over the illuminated area, and cumulative probabilities.

For reasons of comparability with F. Tesche's results [3, 4], the locations of the transmission lines are chosen as in his paper, one near Ground Zero with a ground range of 233.5 km, another near the horizon at a ground range of 2100 km. The height of burst is 400 km, the gamma yield is assumed to be 10 kt. The height of the transmission line is  $h = 10$  m (unless

otherwise stated). It should be observed that the two selected positions are not those of maximum line response. This will rather occur at a ground range of 1040 km ( $R = 2.6$ ) and an observer location azimuth angle  $\phi = -5^\circ$  measured as being negative in clockwise direction from the east. For a 200 km burst the polar coordinates of the corresponding position are  $R = 3.64$ ,  $\phi = -6.7^\circ$ .

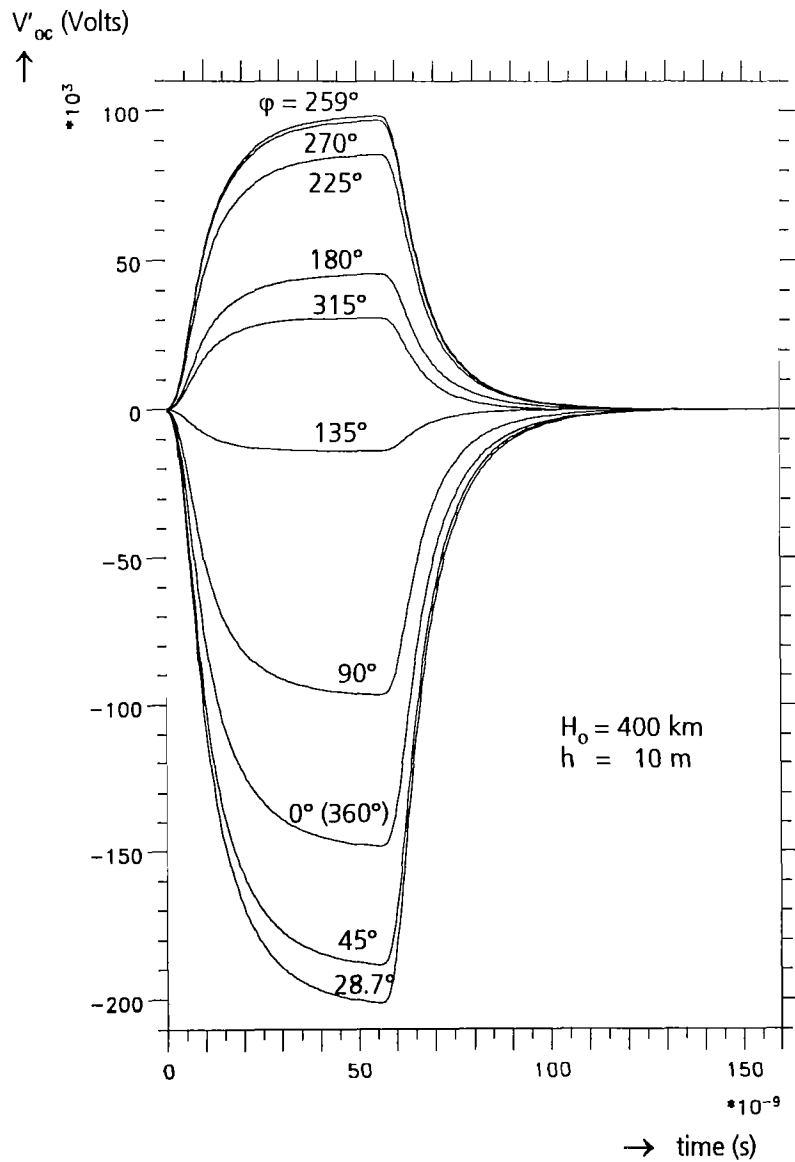
Figures 1 and 2 show the induced open-circuit voltages as a function of time for different line orientation or azimuthal angles  $\phi$  for a line located near Ground Zero. Figure 1 refers to (6), i.e. considers only the contribution  $V'_{oc}$  of the horizontal line, whereas Figure 2 includes the vertical potential difference (shown as the dashed curve) at the end of the line according to (10). In both figures the envelopes are calculated for azimuth angles as given by (17).

Figures 3 and 4 are the corresponding representations for a location near the eastern horizon. In this case of grazing incidence ( $\psi = 0.93^\circ$ ), the interaction with the horizontal line is negligible for azimuth angles in the range between  $45^\circ$  and  $315^\circ$ . Nevertheless, the open-circuit voltage can amount to 150 kV if the vertical potential difference or a vertical riser element is taken into account. Then the interaction is predominantly caused by the vertical component of the vertically polarized electromagnetic wave.

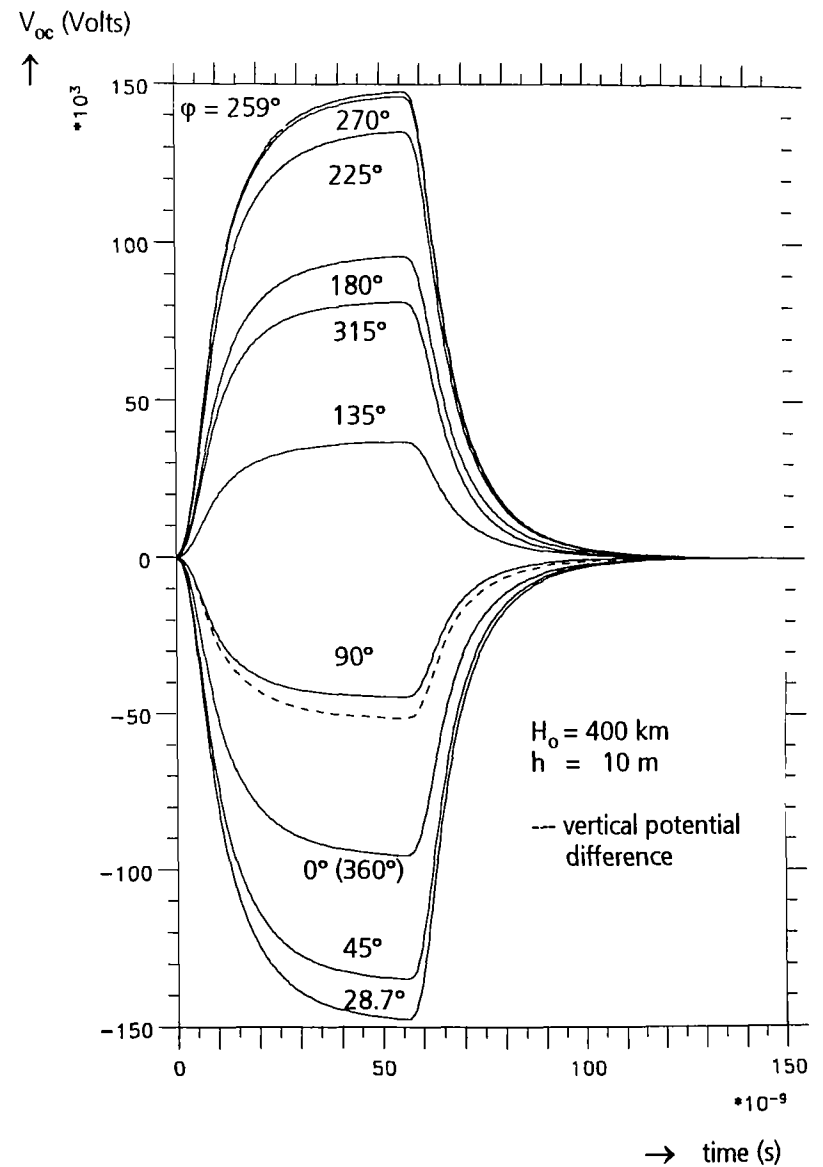
Because the voltage pulse in Figures 3 and 4 lasts only for about 300 ns, only line elements with  $z \gtrsim -100$  m contribute to  $V_{oc}$  at  $z = 0$ . This is due to the complete annihilation of incident and ground-reflected fields in case of a perfectly conducting ground. In this case, the variation of the elevation angle  $\psi$  along the line can be neglected. This might no longer be justified for finite ground conductivities which tend to increase the pulse duration. It is noticed that no positive spikes as discussed in [3, 4] can be found in Figures 2 and 4, because both the horizontally and vertically polarized waves have identical time dependence.

As mentioned above, considerably higher voltages can be obtained for line locations different from those discussed previously. Figures 5 and 6 show the results for  $R = 3.64$ ,  $\phi = -6.7^\circ$  (see also Table I and Figure 15).

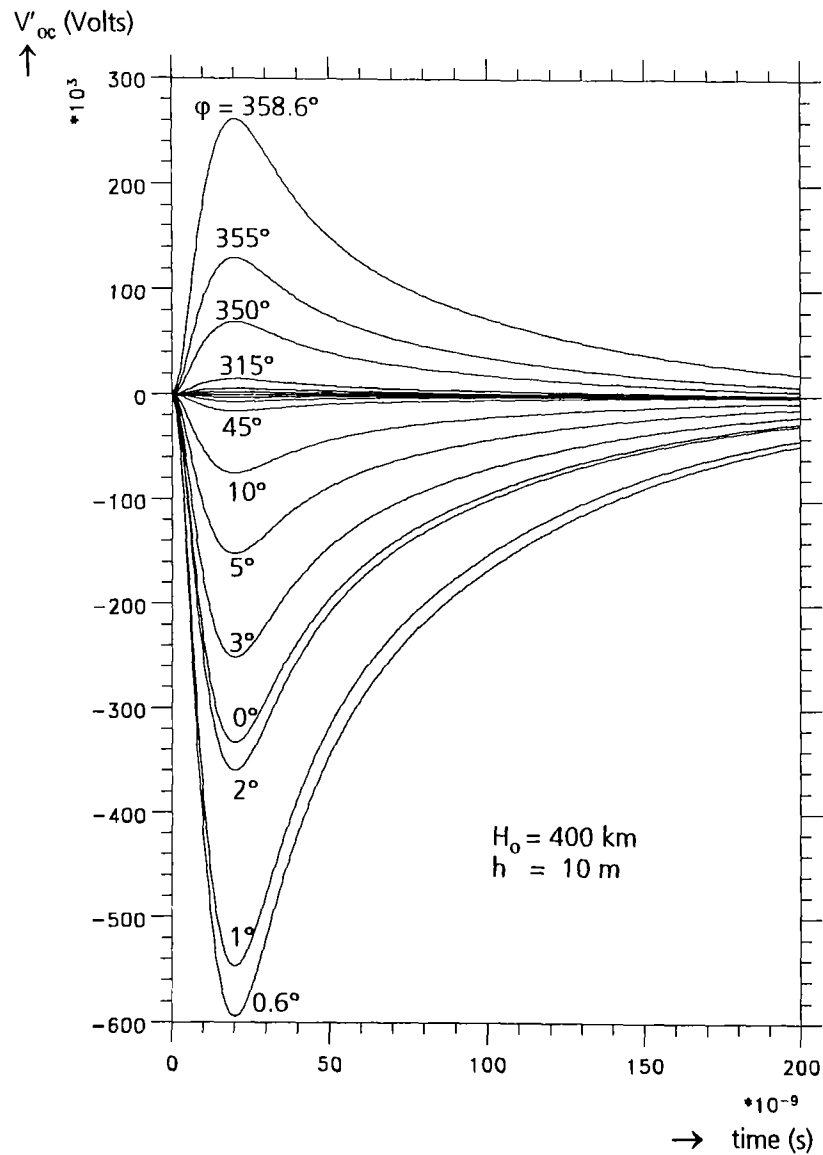
Figures 7 to 9 are polar plots of the peak voltages of the voltage pulses corresponding to Figures 2, 4 and 6. The asymmetry between negative and positive voltages is a measure for the contribution of the vertically polarized wave. Figure 10 is an example of interaction with a horizontally polarized wave as encountered at the location of maximum peak electric field south of Ground Zero.



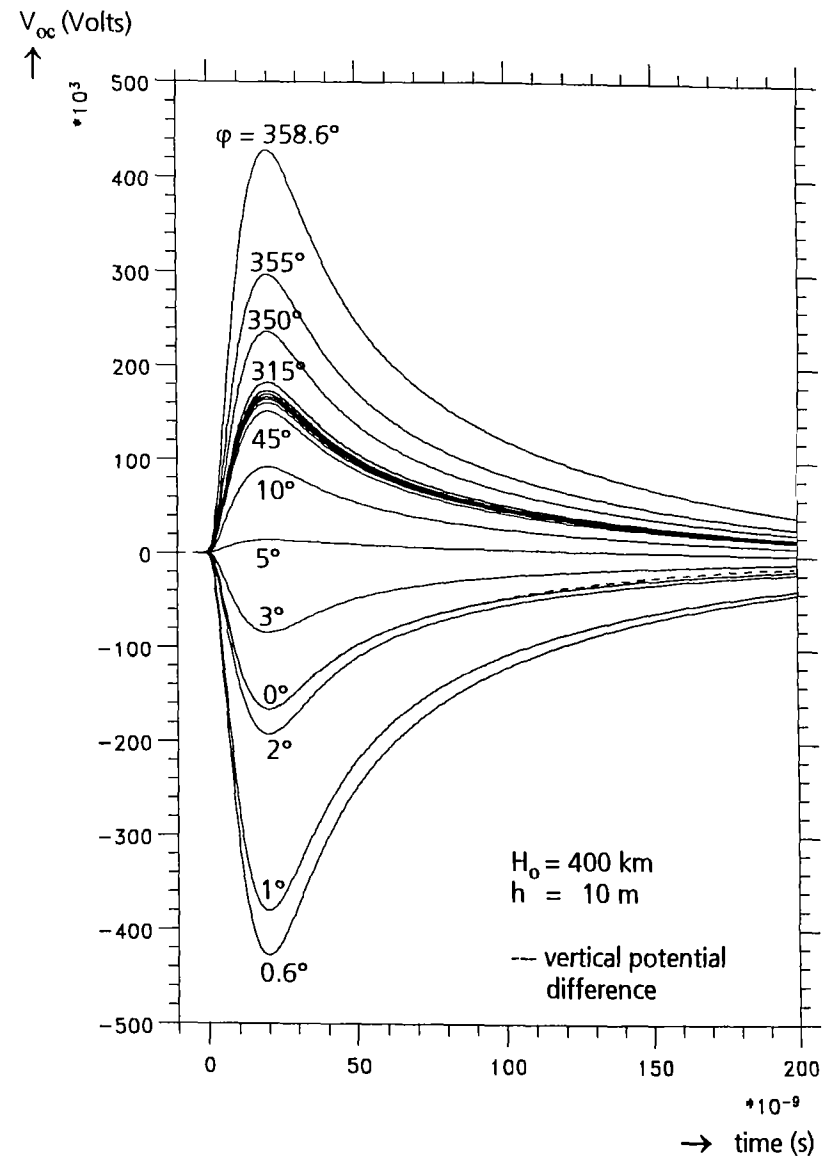
**Figure 1**  
 Open-circuit voltages at the end of a semi-infinite horizontal line for various line orientation angles  $\phi$  at  $R = 233.5$  km,  $\phi = 0^\circ$



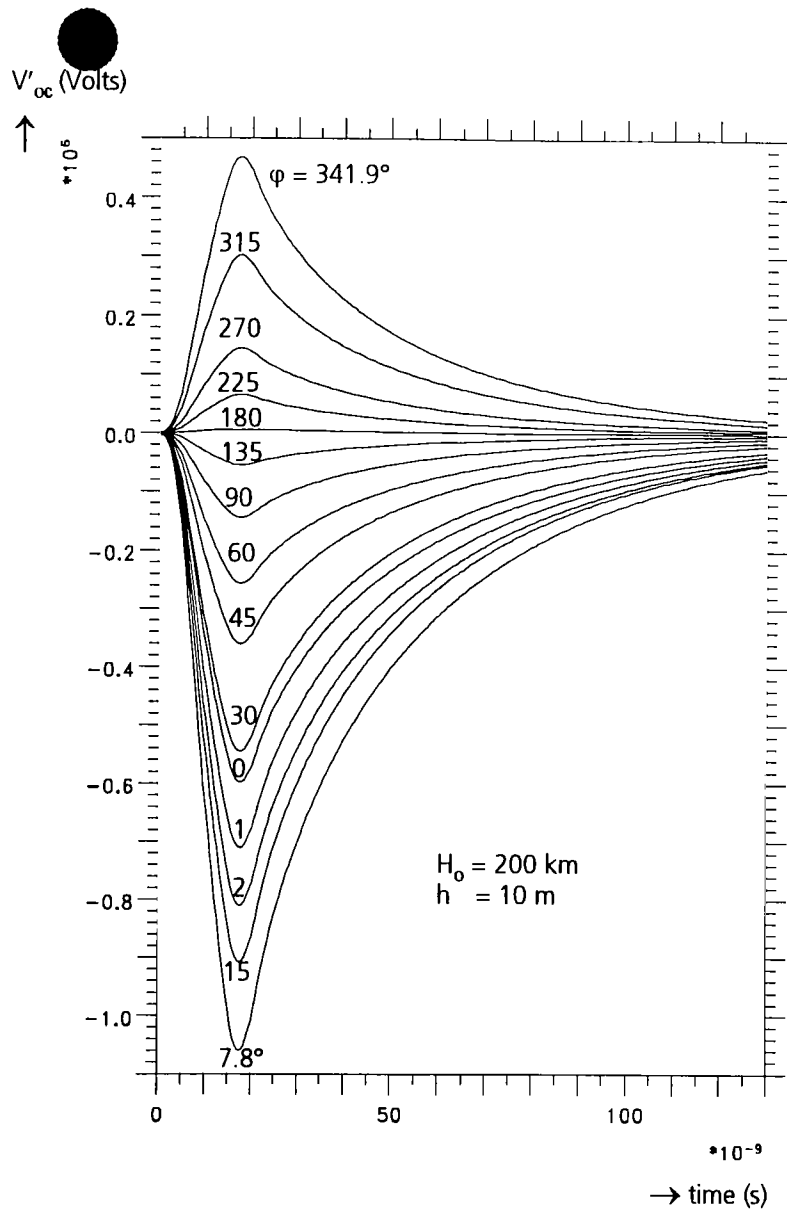
**Figure 2**  
 Open-circuit voltages (including potential difference between horizontal line and ground) for various line orientation angles  $\phi$  at  $R = 233.5$  km,  $\phi = 0^\circ$



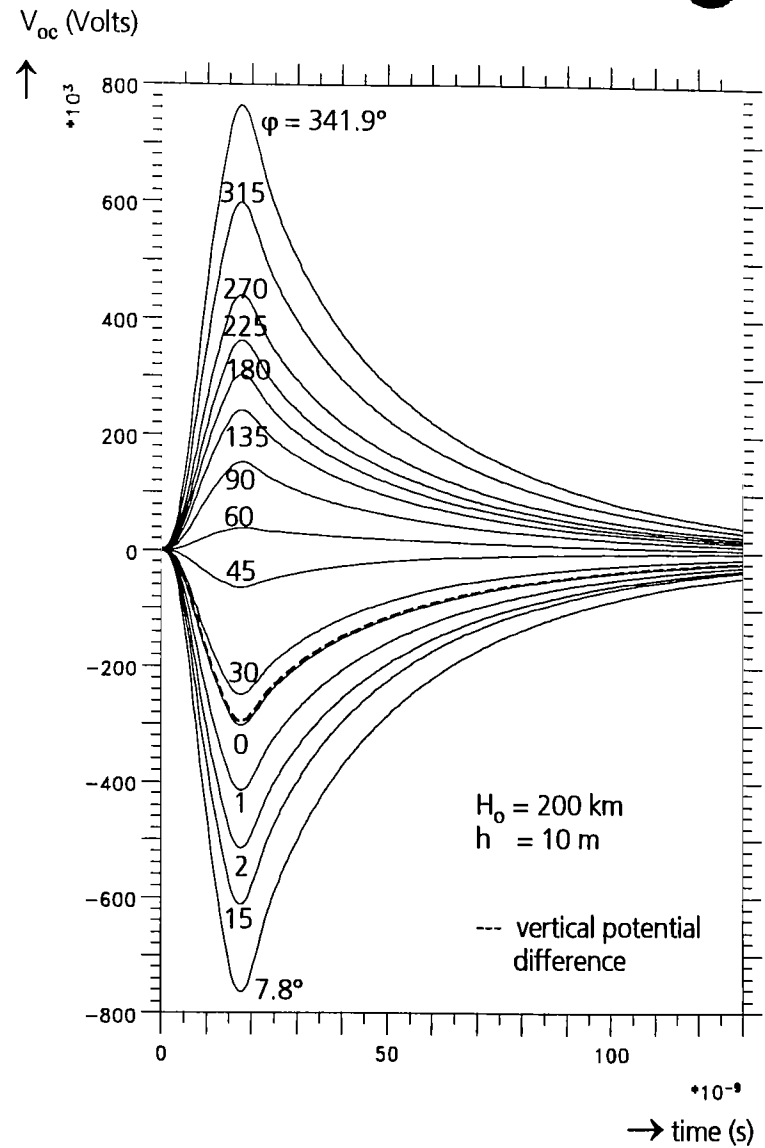
**Figure 3**  
 Open-circuit voltages at the end of a semi-infinite horizontal line for various line orientation angles  $\phi$  near the eastern horizon ( $R = 2100$  km,  $\phi = 0^\circ$ )



**Figure 4**  
 Open-circuit voltages (including potential difference between horizontal line and ground) for various line orientation angles  $\phi$  near the eastern horizon ( $R = 2100$  km,  $\phi = 0^\circ$ )

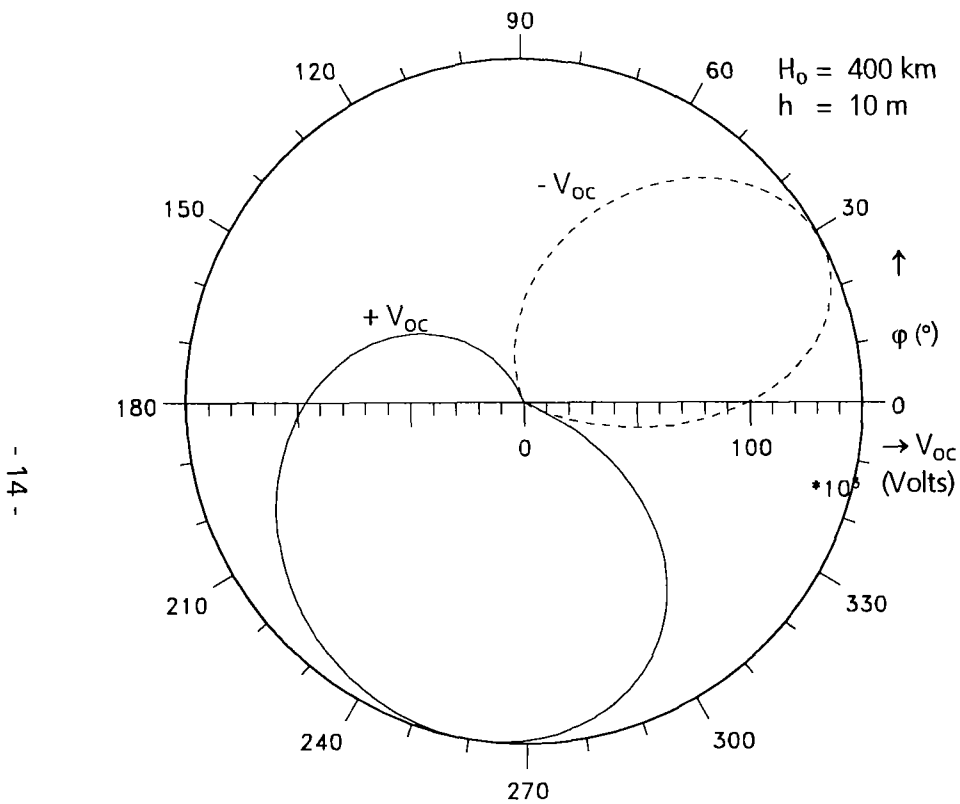


**Figure 5**  
**Open-circuit voltages at the end of a semi-infinite horizontal line for various line orientation angles  $\phi$  at the location of maximum response ( $R = 3.64 \times H_0 = 728$  km,  $\phi = -6.7^\circ$ )**

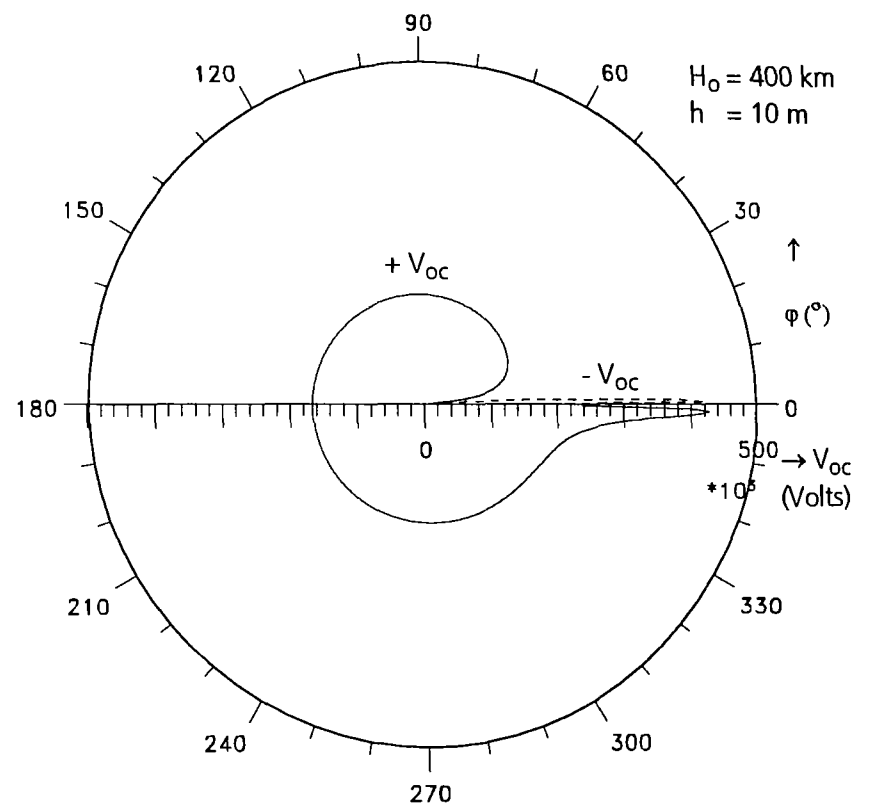


**Figure 6**  
**Open-circuit voltages (incl. vertical potential difference) for various line orientation angles  $\phi$  at the location of maximum response ( $R = 3.64 \times H_0 = 728$  km,  $\phi = -6.7^\circ$ )**

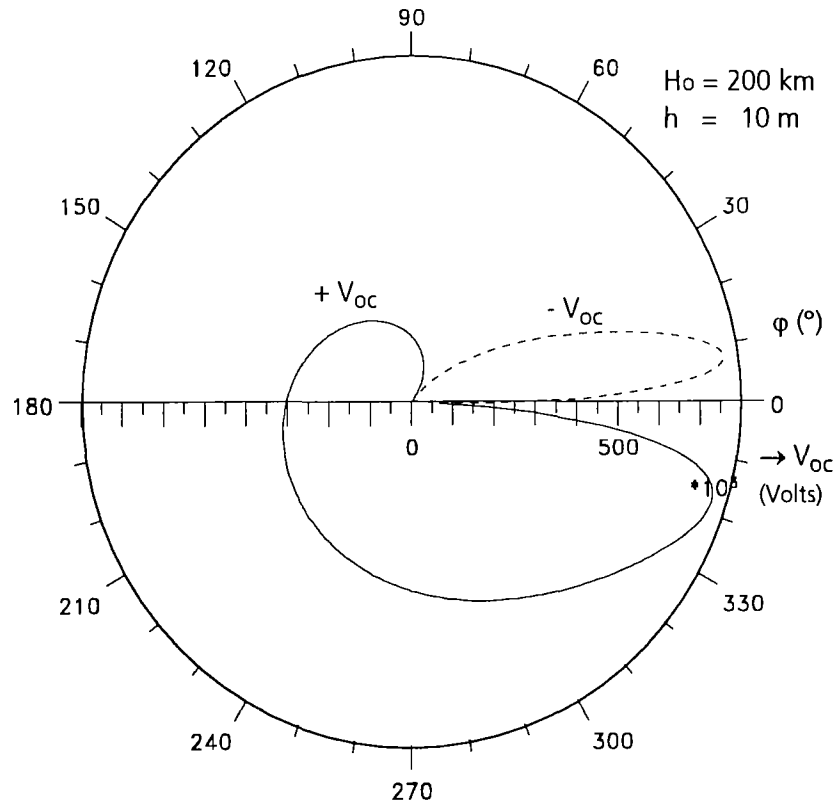




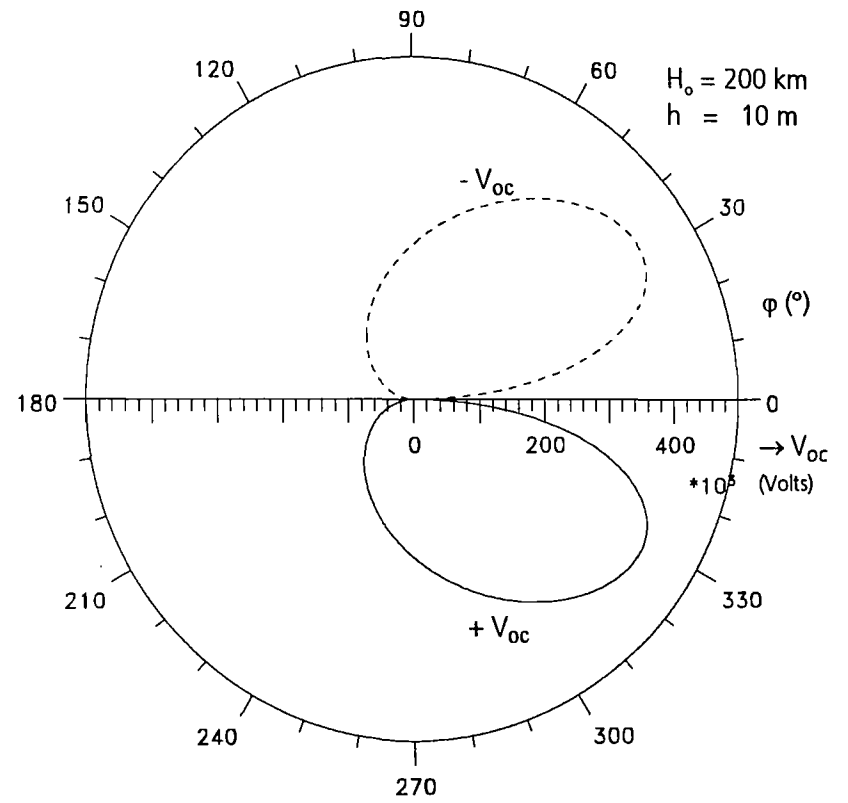
**Figure 7**  
Peak open-circuit voltages  $V_{OC}$  as a function of line orientation angle  $\phi$  at the location  $R = 233.5 \text{ km}$ ,  $\phi = 0^{\circ}$



**Figure 8**  
Peak open-circuit voltages  $V_{OC}$  as a function of line orientation angle  $\phi$  near the horizon eastward of Ground Zero ( $R = 2100 \text{ km}$ ,  $\phi = 0^{\circ}$ )



**Figure 9**  
 Peak open-circuit voltages  $V_{OC}$  as a function of line orientation angle  $\phi$  at the location of maximum response ( $R = 3.64 \times H_0 = 728$  km,  $\phi = -6.7^\circ$ )



**Figure 10**  
 Peak open-circuit voltages  $V_{OC}$  as a function of line orientation angle  $\phi$  at the location of maximum peak electric field magnitude ( $R = 1.4 \times H_0 = 280$  km,  $\phi = -90^\circ$ )

Figures 11 to 14 are contour plots showing the peak voltages for each line location within the illuminated area. In Figure 11, all "semi-infinite" transmission lines are oriented in west-east direction with the open front-end directed to the east. The highest voltages occur for "end-on" incidences ( $\varphi < 90^\circ$ ) in the eastern half-plane, whereas coupling remains small for "front-on" incidences ( $\varphi > 90^\circ$ ) in the western half-plane. The vertical potential difference is included in Figure 12. Comparing both figures shows that near the horizon and also in the western half-plane the contributions of the vertically polarized wave dominate. Figures 13 and 14 refer to transmission lines extended in south-north and in north-south directions, respectively.

In Figures 15 and 16, the local azimuth angle  $\varphi$  is chosen such that maximum response is achieved. The two plots are calculated for gamma yields of 10 kt and 1 kt, respectively. With decreasing yield, the area of maximum coupling migrates from east or west towards south of Ground Zero.

This is also the case for decreasing height  $h$  of the transmission line as shown in Table I, which lists maximum peak voltages, their respective locations ( $R, \phi$ ) in polar coordinates, and elevation angles  $\psi$  as well as mean voltages when averaged over the entire coverage area. The gamma yield is 10 kt.

$h$ (m)	$V_{oc, max}$ (kV)	$\langle V \rangle_{av}$ (kV)	$R$	$\phi$ ( $^\circ$ )	$\psi$ ( $^\circ$ )
0.5	58	38	1.53	- 89.5	31.4
1	111	75	1.79	- 77.8	27.2
2	205	145	2.28	- 40.0	21.3
5	440	342	2.95	- 19.5	15.8
10	764	630	3.64	- 6.7	11.9
15	1045	887	4.09	0.1	9.8

**Table I** *Locations of maximum peak open-circuit voltages in polar coordinates  $R$  (in terms of a  $H_0 = 200$  km burst) and  $\phi$  ( $\phi = 0^\circ \hat{=}$  eastern direction).  $\psi$  is the corresponding elevation angle of the propagation vector of the incident wave.*


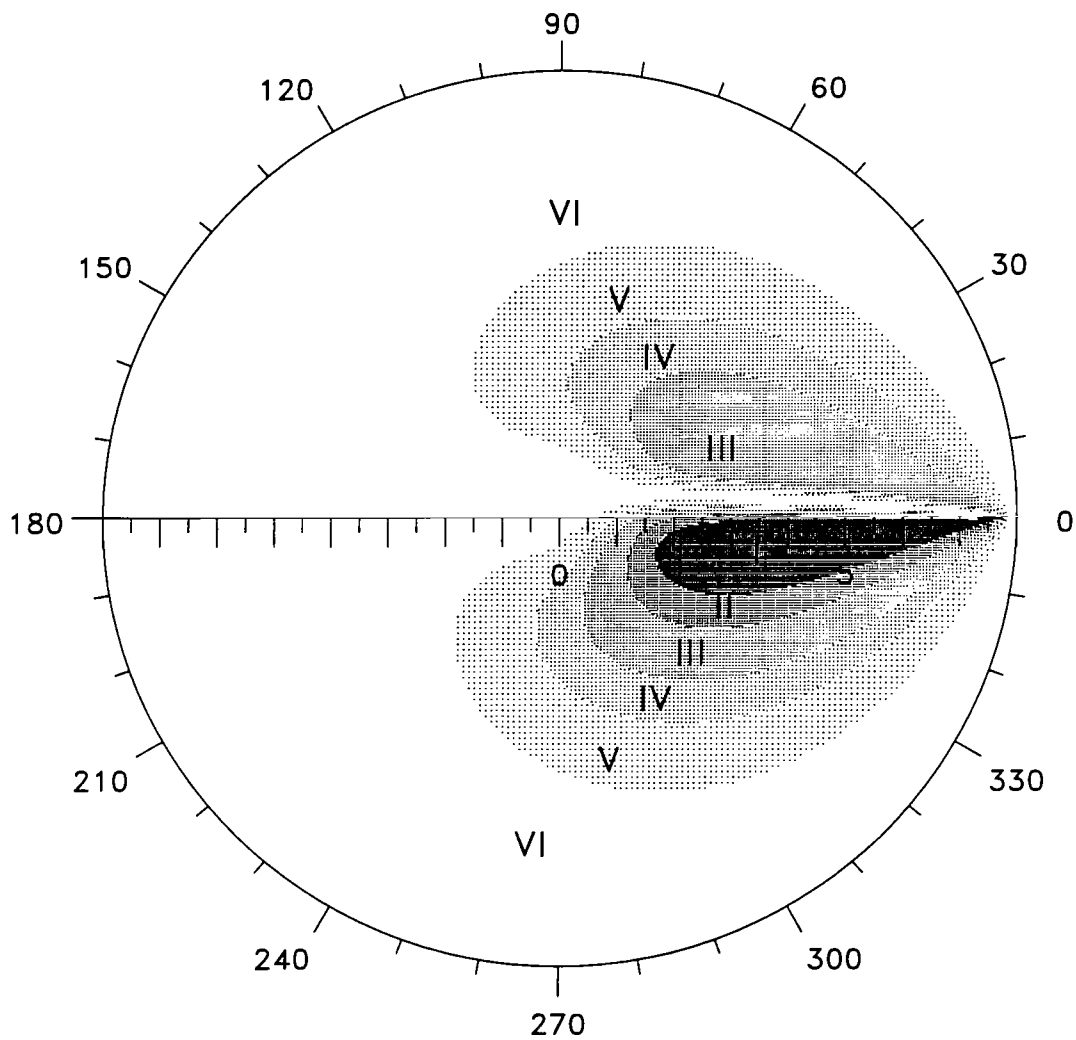


Figure 17 shows corresponding data also for lower yields.

The following four diagrams are devoted to cumulative probabilities of open-circuit voltages which were obtained under the assumption that the transmission lines are uniformly distributed over the entire illuminated area.

Figures 18 and 19 (for  $Y_\gamma = 10$  kt and 1 kt, respectively) are obtained when the local line orientation or azimuth angle is such that  $\varphi = \varphi_{\max}$ . Figure 20 is the result for a random distribution of  $\varphi$  at each position within the illuminated area, whereas in Figure 21 all transmission lines are oriented in west-east direction, i.e.  $\varphi = \phi$ .

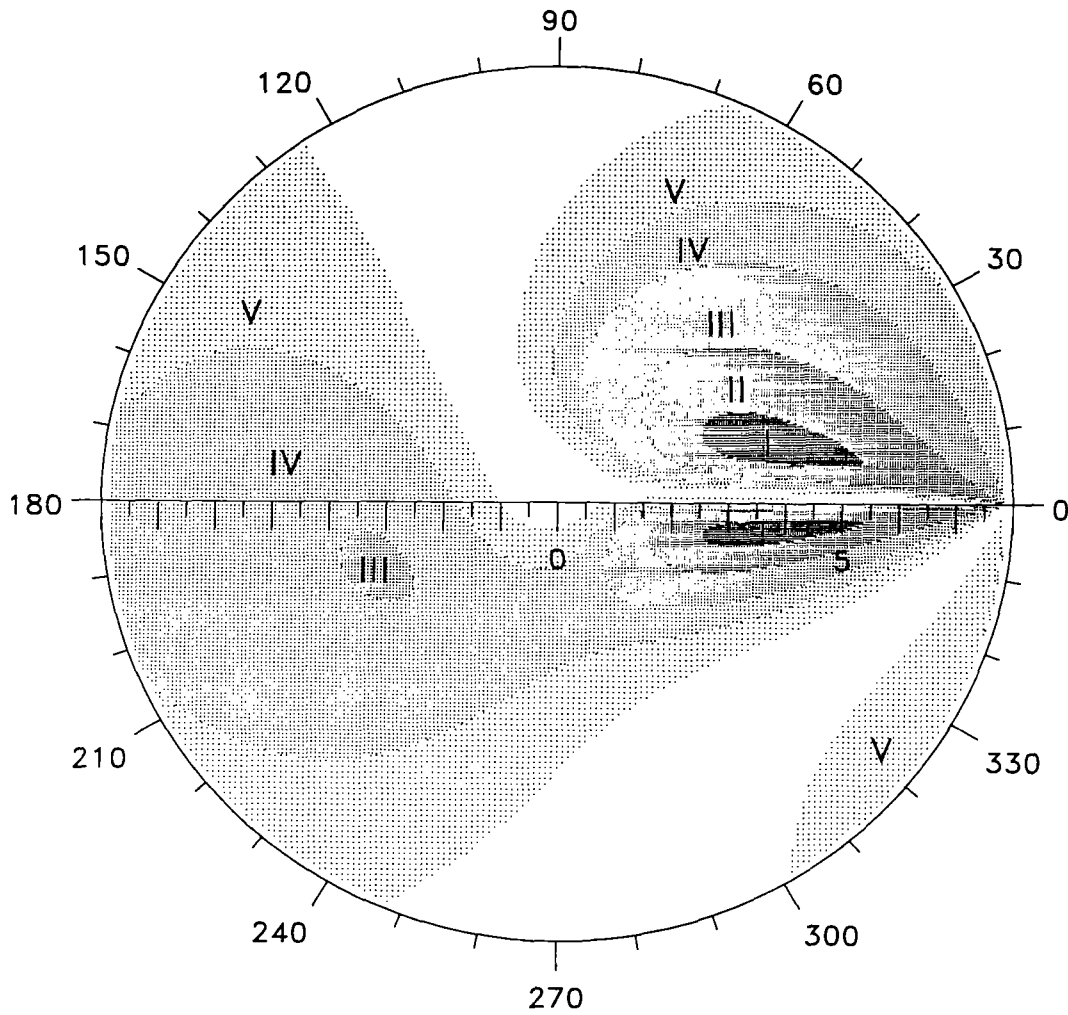


**Figure 11**

**Contour plot of the peak open-circuit voltages  $V'_{oc, pk}$  induced in semi-infinite horizontal lines in west-east direction.**

**( $H_o = 200 \text{ km}$ ,  $h = 10 \text{ m}$ )**

- I: 0.70 - 1.04 MV
- II: 0.50 - 0.70 MV
- III: 0.30 - 0.50 MV
- IV: 0.20 - 0.30 MV
- V: 0.10 - 0.20 MV
- VI: 0.00 - 0.10 MV

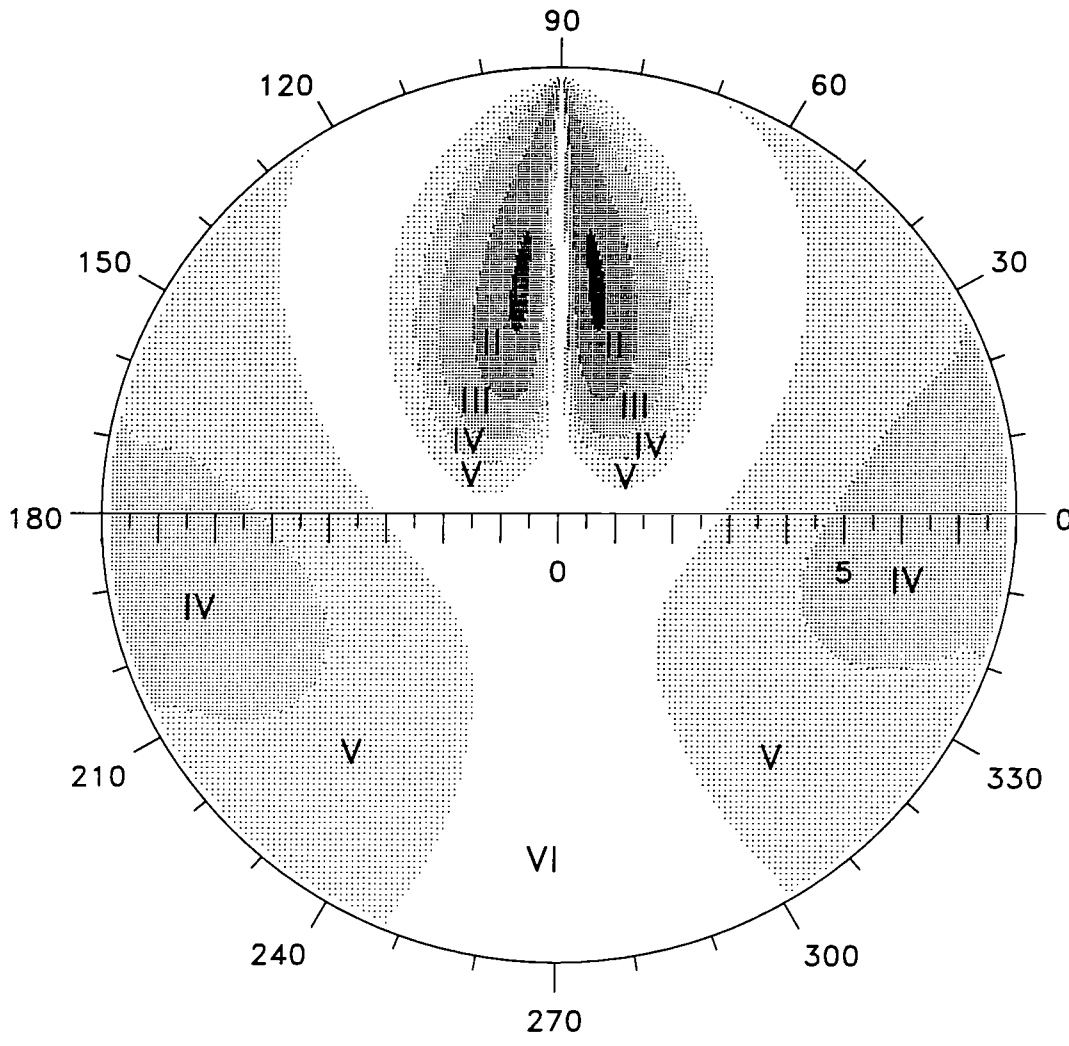


**Figure 12**

*Contour plot of peak open-circuit voltages  $V_{OC, pk}$  (including vertical potential differences) induced in semi-infinite horizontal lines in west-east direction.*

*( $H_o = 200 \text{ km}$ ,  $h = 10 \text{ m}$ )*

- I: 0.70 - 0.75 MV
- II: 0.50 - 0.70 MV
- III: 0.30 - 0.50 MV
- IV: 0.20 - 0.30 MV
- V: 0.10 - 0.20 MV
- VI: 0.00 - 0.10 MV

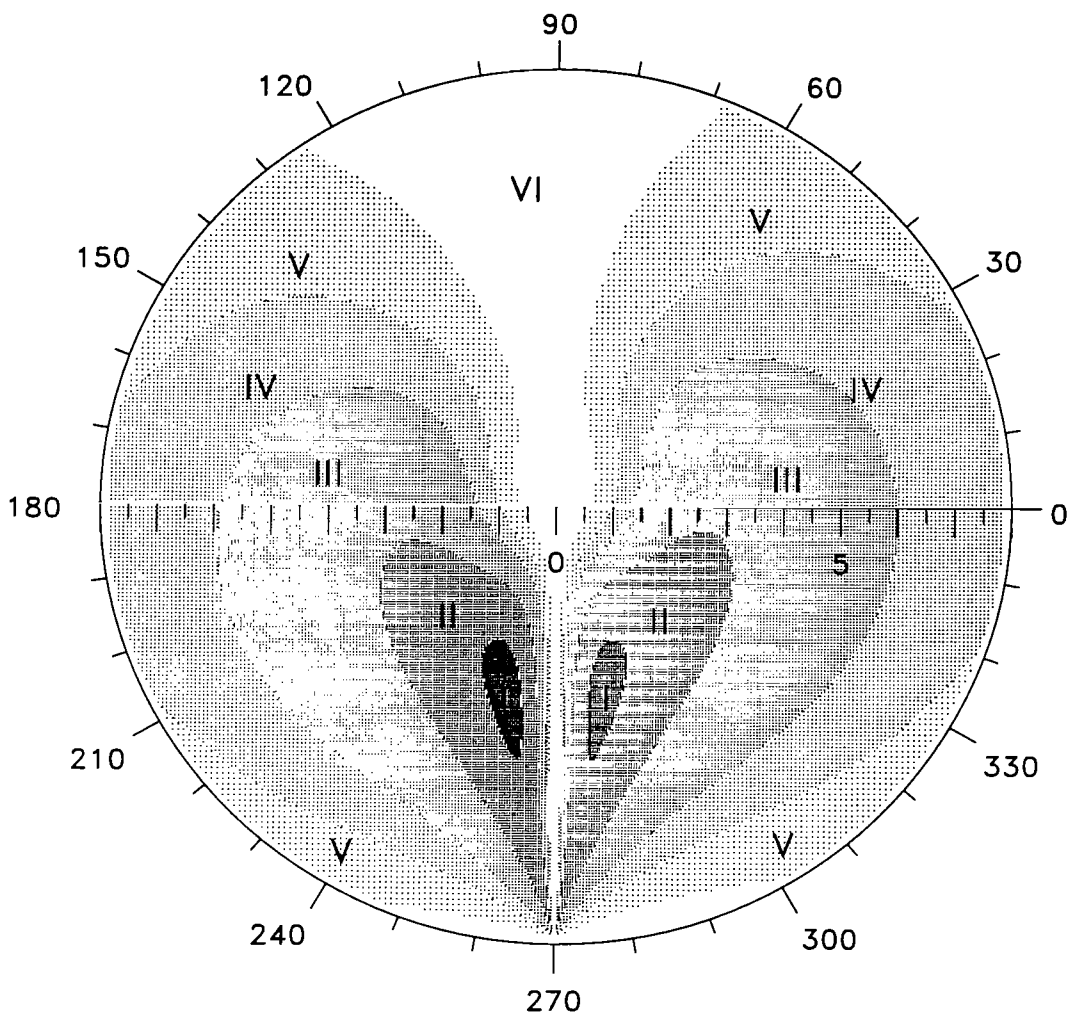


**Figure 13**

*Contour plot of the peak open-circuit voltages  $V_{oc, pk}$  (including vertical potential differences) induced in semi-infinite horizontal lines in south-north direction.*

*( $H_o = 200$  km,  $h = 10$  m)*

- I: 0.70 - 0.75 MV
- II: 0.50 - 0.70 MV
- III: 0.30 - 0.50 MV
- IV: 0.20 - 0.30 MV
- V: 0.10 - 0.20 MV
- VI: 0.00 - 0.10 MV



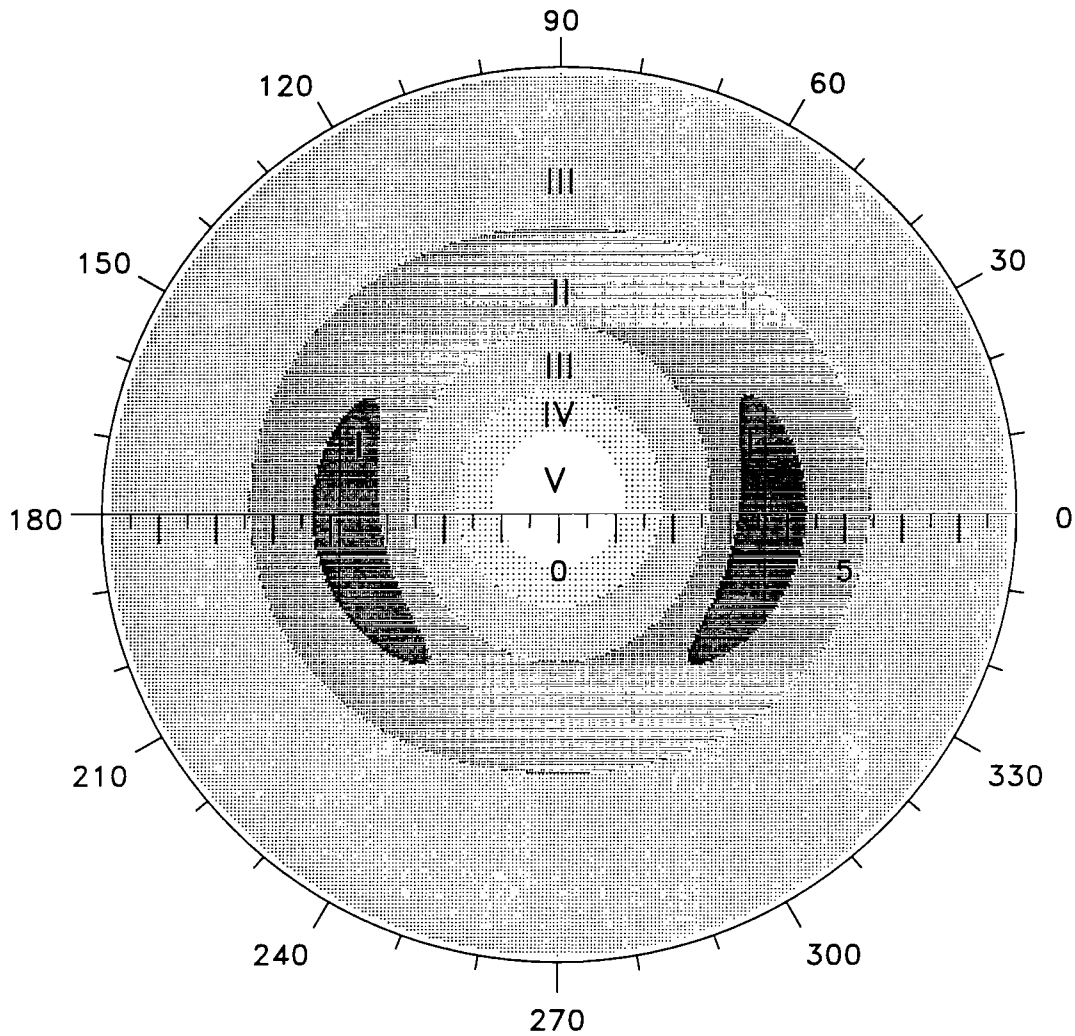
**Figure 14**

**Contour plot of peak open-circuit voltages  $V_{OC, pk}$  induced in semi-infinite horizontal lines in north-south direction.**

**( $H_o = 200$  km,  $h = 10$  m)**

- I: 0.70 - 0.75 MV
- II: 0.50 - 0.70 MV
- III: 0.30 - 0.50 MV
- IV: 0.20 - 0.30 MV
- V: 0.10 - 0.20 MV
- VI: 0.00 - 0.10 MV



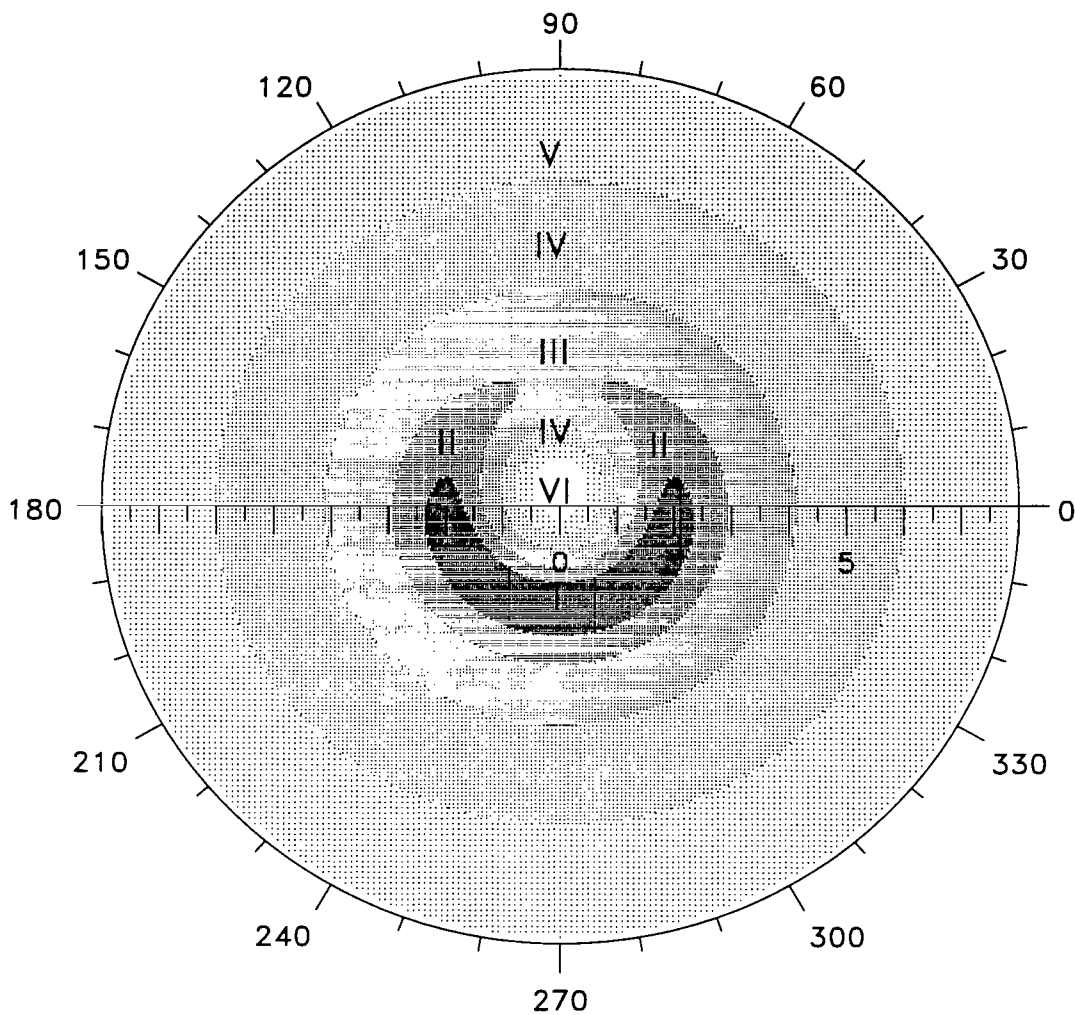


**Figure 15**

*Contour plot of  $V_{max}$  (as obtained from Eq. 20) for the local azimuth angle  $\varphi = \varphi_{max}$  and a gamma yield of 10 kt.*

*( $H_o = 200$  km,  $h = 10$  m)*

- I: 0.75 - 0.76 MV
- II: 0.70 - 0.75 MV
- III: 0.50 - 0.70 MV
- IV: 0.25 - 0.50 MV
- V: 0 - 0.25 MV

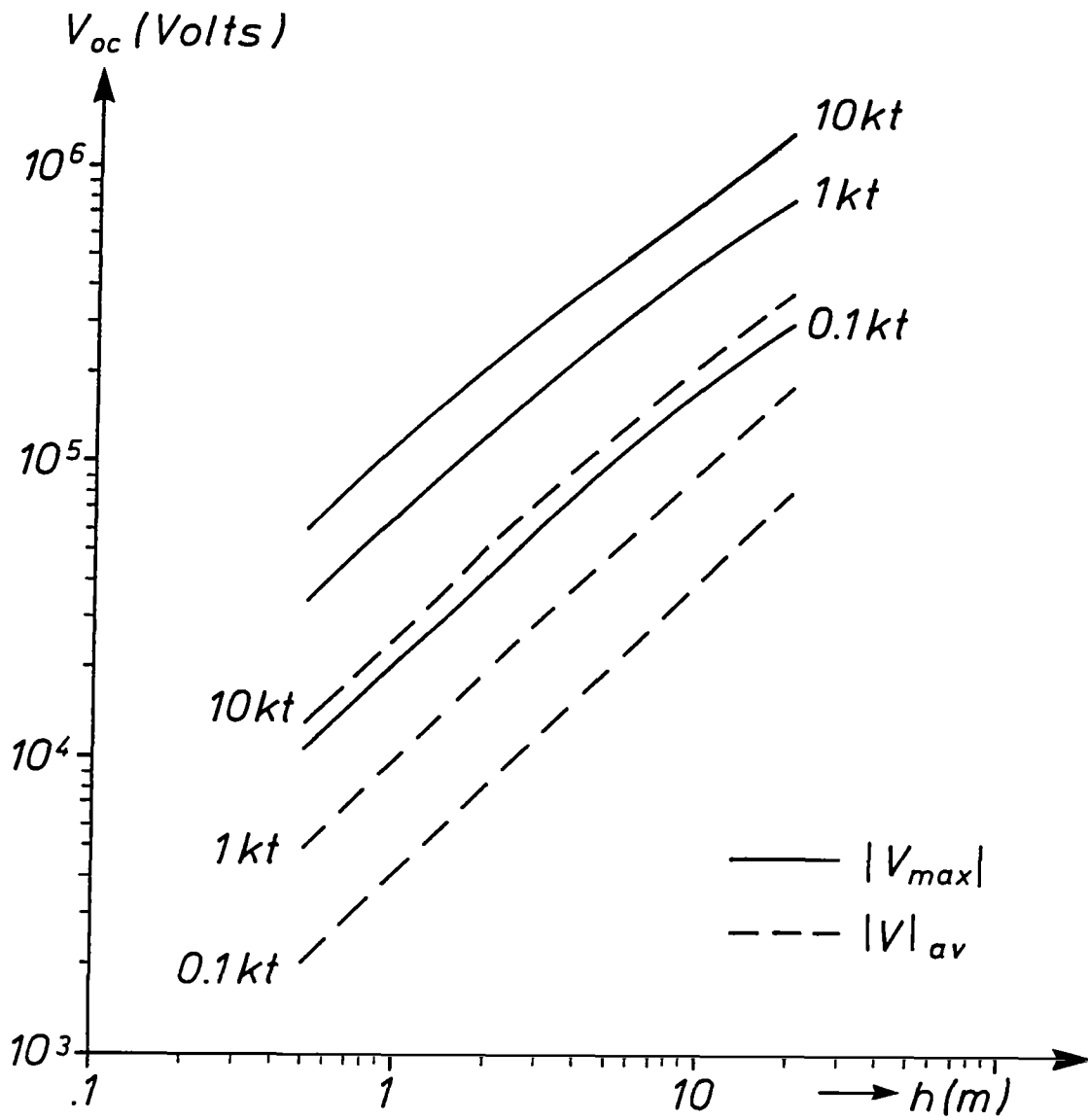


**Figure 16**

*Contour plot of  $V_{max}$  (as obtained from Eq. 20) for the local azimuth angle  $\phi = \phi_{max}$  and a gamma yield of 1 kt.*

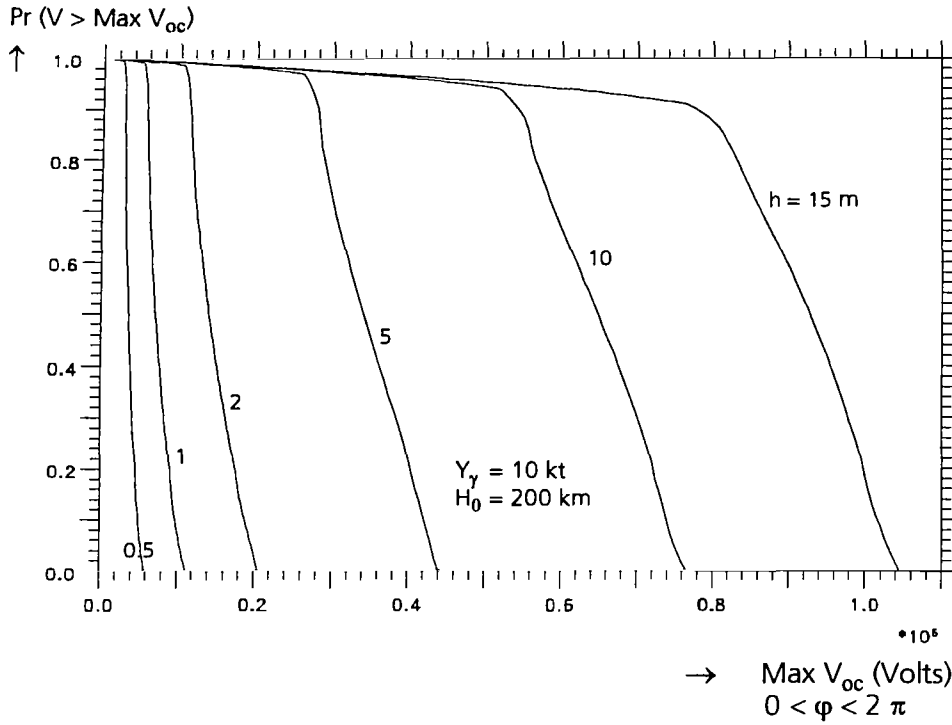
*( $H_o = 200$  km,  $h = 10$  m)*

I:	0.45 - 0.48 MV
II:	0.40 - 0.45 MV
III:	0.30 - 0.40 MV
IV:	0.20 - 0.30 MV
V:	0.10 - 0.20 MV
VI:	0 - 0.10 MV

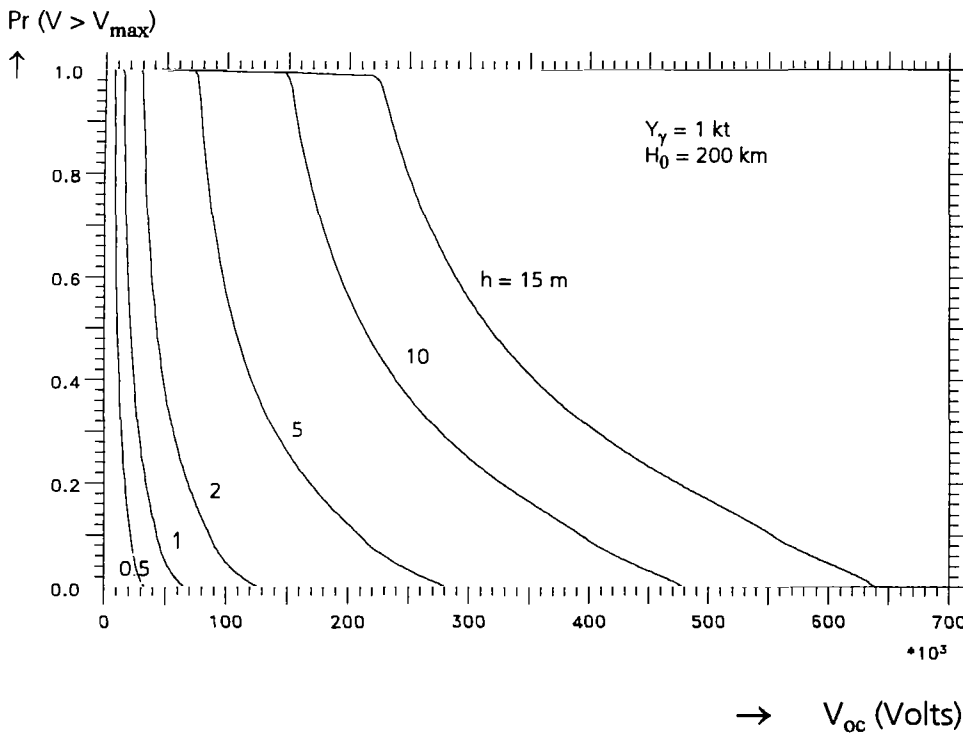


**Figure 17**

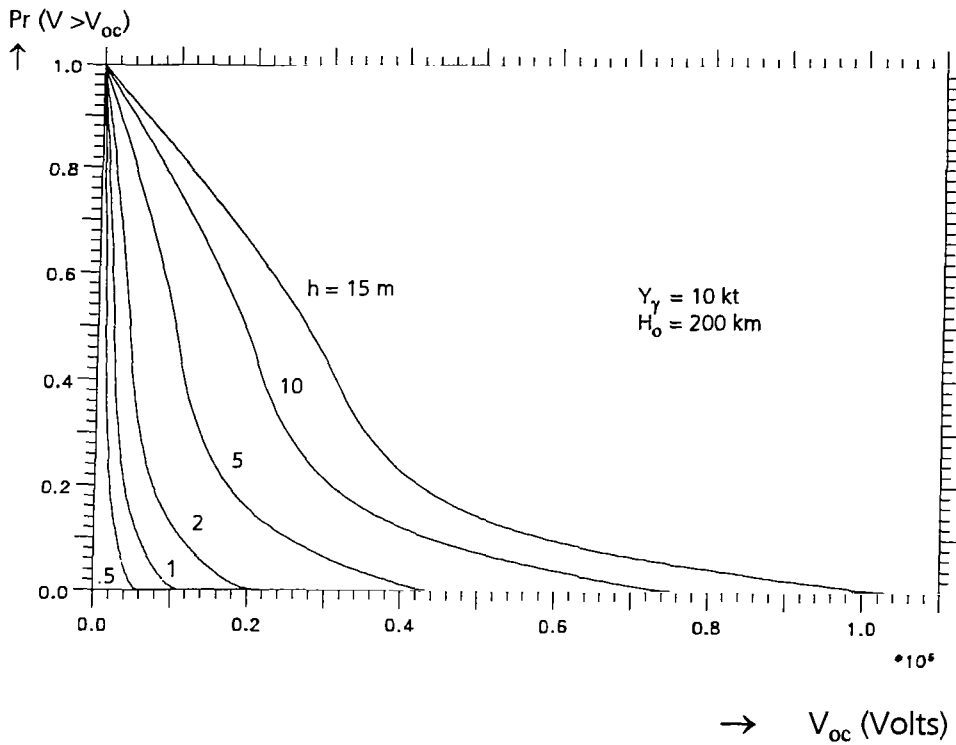
*Maximum and average peak open-circuit voltages of semi-infinite transmission lines as a function of height  $h$  over ground and gamma yield  $\gamma$*



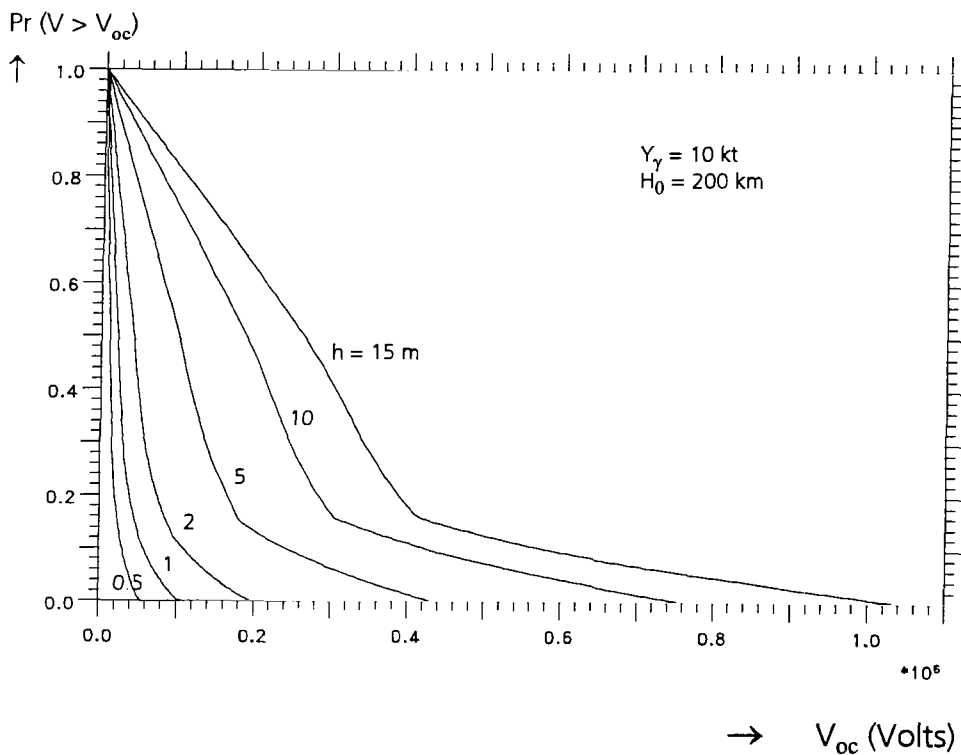
**Figure 18**  
**Cumulative probabilities of positive peak open-circuit voltages for the line orientation angle  $\varphi_{max}$  of maximum response ( $Y_\gamma = 10 \text{ kt}$ )**



**Figure 19**  
**Cumulative probabilities of positive peak open-circuit voltages for the line orientation angle  $\varphi_{max}$  of maximum response ( $Y_\gamma = 1 \text{ kt}$ )**



**Figure 20**  
*Cumulative probabilities of positive peak open-circuit voltages for random line orientation angles  $\varphi$*

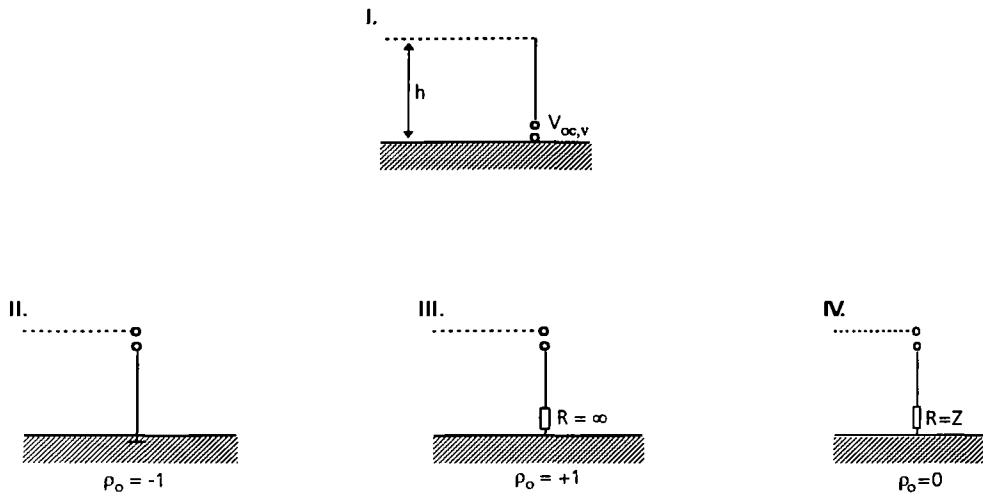


**Figure 21**  
*Cumulative probabilities of positive peak open-circuit voltages for a transmission line oriented in west-east direction*

#### 4. Coupling to Vertical Line Elements

This section particularly deals with the HEMP interaction with vertical elements. Because only the vertical component of the electric field vector, i.e. the vertical component of the vertically polarized incident electromagnetic wave, is responsible for coupling, the interaction is independent of the azimuth angle  $\varphi$ .

The interaction depends on the manner a vertical element of length  $h$  between the ground and a horizontal line of height  $h$  is terminated at its ends. Four different cases will be considered.



- I. The open-circuit voltage is calculated at the base of the vertical element terminated at its top in its characteristic wave impedance (i.e. the vertical line is connected to a semi-infinite horizontal line such that no reflections from the upper end occur).
- II. The open-circuit voltage is calculated at the upper end of the vertical element whose lower end is short-circuited to a perfectly conducting ground such that the reflection coefficient of the induced current pulse traveling downward becomes  $\rho_o = -1$ .
- III. The open-circuit voltage is calculated at the upper end. The base is not connected to ground (i.e. terminated by a resistor or load impedance  $R = \infty$ ). Hence, the reflection coefficient at the base is  $\rho_o = +1$ .
- IV. Again, the open-circuit voltage is calculated at top. The base is terminated in its characteristic impedance, and therefore  $\rho_o = 0$ .

In correspondence to horizontal lines, induced current pulses and open-circuit voltages are calculated by consistent application of the rules of transmission line theory despite the fact that this theory is limited to electrically small heights, and radiation losses are not taken into account. Hence, a more rigorous treatment should result in deviations in particular for higher frequencies determined by the rising part of the incident and ground-reflected HEMP. However, even then transmission line theory may provide a satisfactory estimate [10].

Since the ground is assumed to be perfectly conducting in this paper, the interaction can be calculated in time-domain. This has the advantage that the time-domain HEMP as calculated by the EXEMP code does not require transformation into the frequency-domain prior to the interaction calculation.

For all types of vertical elements it will be assumed that  $t = 0$  is defined by the time where the wave front first arrives at the top of the vertical element.

For case (I), the open-circuit voltage at the base is then given by

$$\begin{aligned}
 V_{oc,v}(t) &= \cos \psi \int_0^h E_v \left( t - \frac{h-x}{c} \sin \psi - \frac{x}{c} \right) dx + \cos \psi \int_0^h E_v \left( t - \frac{h+x}{c} \sin \psi - \frac{x}{c} \right) dx \\
 &= \frac{\cos \psi}{1 - \sin \psi} c \int_{t-t_0/2}^{t-t_r/2} E_v(t') dt' + \frac{\cos \psi}{1 + \sin \psi} c \int_{t-t_r-t_0/2}^{t-t_r/2} E_v(t') dt' \\
 &\equiv \frac{\cos \psi}{1 - \sin \psi} I_v \left( t; \frac{t_r}{2}, \frac{t_0}{2} \right) + \frac{\cos \psi}{1 + \sin \psi} I_v \left( t; \frac{t_r}{2}, t_r + \frac{t_0}{2} \right)
 \end{aligned} \tag{26}$$

where

$$I_v(t; t_1, t_2) \equiv c \int_{t-t_2}^{t-t_1} E_v(t') dt', \tag{27}$$

$$t_0 = \frac{2h}{c} \quad \text{and} \quad t_r = \frac{2h}{c} \sin \psi.$$

The first term on the right-hand side in Eq. (26) corresponds to the incident wave, the second term to the ground-reflected wave.

Had  $t = 0$  been defined as the time where the wave fronts first arrives at the lower end of the vertical riser, a transformation

$$t \rightarrow t + \frac{t_r}{2}$$

would lead to

$$V_{oc, v}(t) = \frac{\cos \psi}{1 - \sin \psi} I_v \left( t; 0, \frac{t_o - t_r}{2} \right) + \frac{\cos \psi}{1 + \sin \psi} I_v \left( t; 0, \frac{t_o + t_r}{2} \right). \quad (28)$$

Eq. (26) was also obtained in [10] by Fourier transformation of the frequency-domain result. It is noticed that in the present paper  $E(t)$  is defined for negative times, whereas in [10]  $E(t) = 0$  for  $t \leq 0$ .

The cases (II) to (IV) do not require individual treatment. They are only distinguished by the reflection coefficient  $\rho_o$  of the induced current pulse at the lower end.

Four terms contribute to the open-circuit voltage at the upper end

$$\begin{aligned} V_{oc, v}(t) = \cos \psi \sum_{n=0}^{\infty} \rho_o^n & \left\{ \int_0^h E_v \left( t - \frac{h-x}{c} \sin \psi - \frac{1}{c} ((2n+1)h-x) \right) dx \right. \\ & - \rho_o \int_0^h E_v \left( t - \frac{h-x}{c} \sin \psi - \frac{1}{c} ((2n+1)h+x) \right) dx \\ & + \int_0^h E_v \left( t - \frac{h+x}{c} \sin \psi - \frac{1}{c} ((2n+1)h-x) \right) dx \\ & \left. - \rho_o \int_0^h E_v \left( t - \frac{h+x}{c} \sin \psi - \frac{1}{c} ((2n+1)h+x) \right) dx \right\}. \quad (29) \end{aligned}$$

The first term results from the current pulse traveling upward, being reflected at the upper open end with a reflection coefficient  $+1$ , traveling downward, being reflected at the lower end with a reflection coefficient  $\rho_o$ , and so forth.

The second term results from the pulse traveling in the opposite direction with negative sign, i.e. starting downward. Its first reflection will occur at the bottom with  $\rho_o$ , and so forth. The third and fourth term result from the corresponding contributions of the ground-reflected wave.



Eq. (29) is rewritten as

$$\begin{aligned}
 V_{oc,v}(t) = & \frac{\cos \psi}{1 + \sin \psi} \sum_{n=0}^{\infty} \rho_o^n \left[ I_v(t; nt_o, T_o + nt_o) + \rho_o I_v(t; t_r + (n+1)t_o, T_o + nt_o) \right] + \\
 & + \frac{\cos \psi}{1 - \sin \psi} \sum_{n=0}^{\infty} \rho_o^n \left[ \rho_o I_v(t; (n+1)t_o, T_o + nt_o) + I_v(t; t_r + nt_o, T_o + nt_o) \right]
 \end{aligned} \tag{30}$$

where  $T_o = t_r / 2 + t_o / 2 = (1 + \sin \psi) \frac{h}{2c}$ .

At the horizon,

$$\lim_{\psi \rightarrow 0} V_{oc,v}(t) = 2 \sum_{n=0}^{\infty} \rho_o^n \left[ I_v(t; nt_o, T_o + nt_o) - \rho_o I_v(t; T_o + nt_o, (n+1)t_o) \right]. \tag{31}$$

This shows that the time dependence of the voltage is determined by the integral over the electric field pulse rather than by the pulse itself as assumed in [3,4].

Case (IV), where the lower end of the vertical element is terminated in its characteristic impedance, is also included in Eq. (29) as a special case

$$\begin{aligned}
 \rho_o &= 0 \\
 \rho_o^n &= \begin{cases} 1 & \text{for } n=0 \\ 0 & \text{for } n>0 \end{cases}
 \end{aligned}$$

such that

$$\begin{aligned}
 V_{oc,v}^{(IV)}(t) &= \frac{\cos \psi}{1 + \sin \psi} I_v(t; 0, T_o) + \frac{\cos \psi}{1 - \sin \psi} I_v(t; t_r, T_o) \\
 &= \frac{2}{\cos \psi} I_v(t; 0, T_o) - \frac{\cos \psi}{1 - \sin \psi} I_v(t; 0, t_r).
 \end{aligned} \tag{32}$$

At the horizon ( $\psi \rightarrow 0$ ,  $t_r \rightarrow 0$ ),

$$V_{oc,v}^{(IV)}(t) = 2 I_v \left( t; 0, \frac{t_0}{2} \right) = 2c \int_{t-t_0/2}^t E_v(t') dt'. \quad (33)$$

To show under which conditions the integral in (33) can be approximated by its integrand, i. e.

$$V_{oc,v}^{(IV)}(t) \approx 2hE_v(t), \quad (34)$$

early times are considered for which

$$E_v(t) \approx E_{0,v} e^{\alpha t}. \quad (35)$$

The approximation (34) is only justified if

$$h \ll \frac{2c}{\alpha}. \quad (36)$$

Actually, this condition provides also the basis for application of transmission line theory. Assuming  $\alpha = 1 \text{ ns}^{-1}$ , it follows that  $h \ll 0.6 \text{ m}$ . Vice versa, for  $h = 10 \text{ m}$  the condition for the time constant  $\alpha$  is  $\alpha \ll 0.06 \text{ ns}^{-1}$ . Hence, the transmission line theory conditions are not satisfied in general during the HEMP rise time. As already mentioned above, more accurate numerical calculations (including radiative losses) would be required for comparison to estimate to errors incurred by application of transmission line theory.

## Numerical Results

Figures 22a and 22b show vertical riser open-circuit voltages for the cases (I) and (IV), as calculated by means of the Equations (26) and (32), respectively. The curves refer to different distances from Ground Zero in eastern direction. Maximum peak voltages of 210 kV and 235 kV, respectively, are obtained at a scaled distance of  $R = 3$  (600 km).

For this particular location, the voltages are also depicted in Figures 23a and 23b for various heights  $h$  of the vertical element.

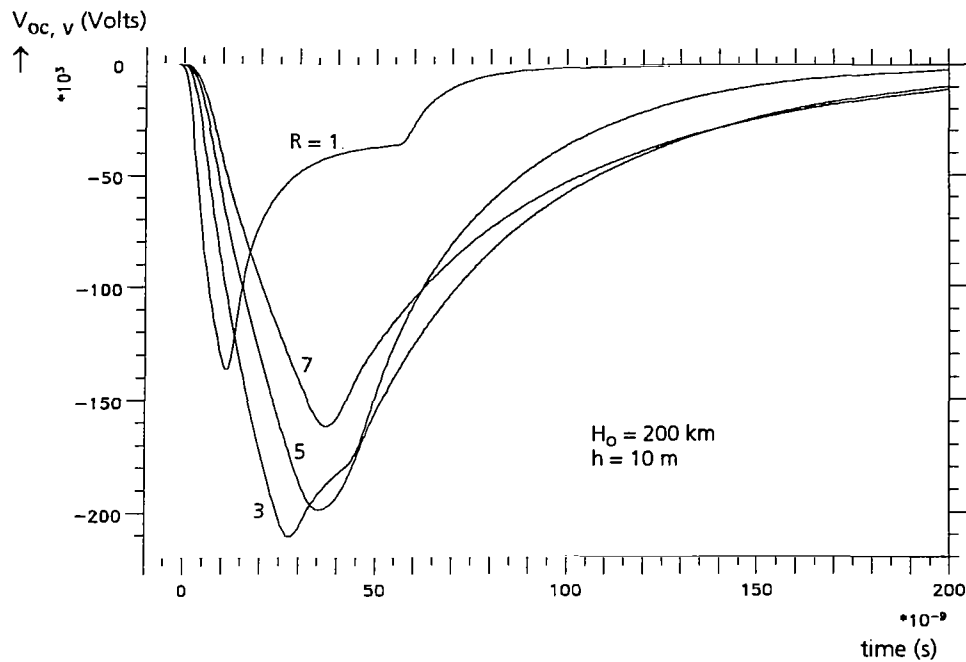
Figure 24 is a contour diagram of the maximum peak voltages in the entire illuminated area as obtained for case (IV). Because the incident electromagnetic wave is horizontally polarized, there is practically no interaction with the vertical line elements in the vicinity of the geomagnetic meridian through Ground Zero. On the other hand, the contributions of vertical riser elements can dominate the interaction with horizontal lines near the horizon, where voltage contributions of up to 200 kV can be expected.

The following Figures 25, 26 and 27 correspond to Figures 2, 4, and 6 with respect to the position within the illuminated area, but with the vertical potential difference replaced by the voltage contribution from vertical elements. The left-hand side plots (a) refer to a vertical riser according to case (I), the right-hand side (b) to case (IV).

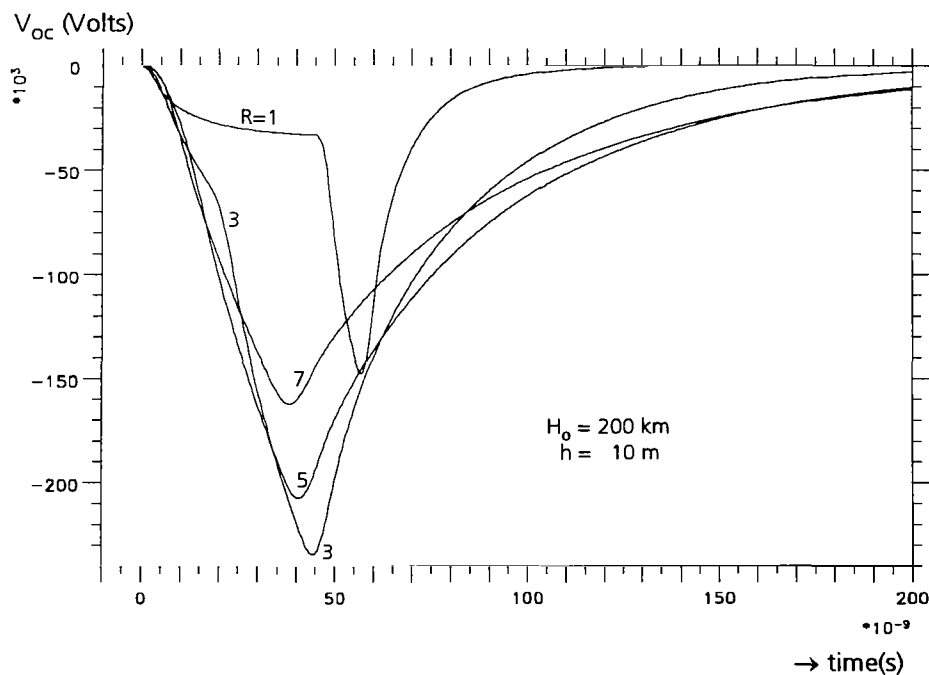
Figures 25a and 25b are examples for the occurrence of positive spikes caused by the vertical elements. However, when the line position moves away from Ground Zero, the spikes are no longer as distinct or even disappear. This fact can easily be explained by observing the  $(1 - \sin\psi)^{-1}$  term in Equations (26) ff.

Figures 28 and 29, corresponding to cases (II) and (III), respectively, are examples for current reflections at the base of the vertical element. Because the reflected pulse traveling upward is again reflected at the top of the element with reflection coefficient  $\rho_o = +1$ , such kinds of vertical elements produce ringing. The oscillation frequency of Figure 29 is twice that of Figure 28 due to the different reflection condition at the base, whereas the configuration presented in Figure 28 produces higher amplitudes.

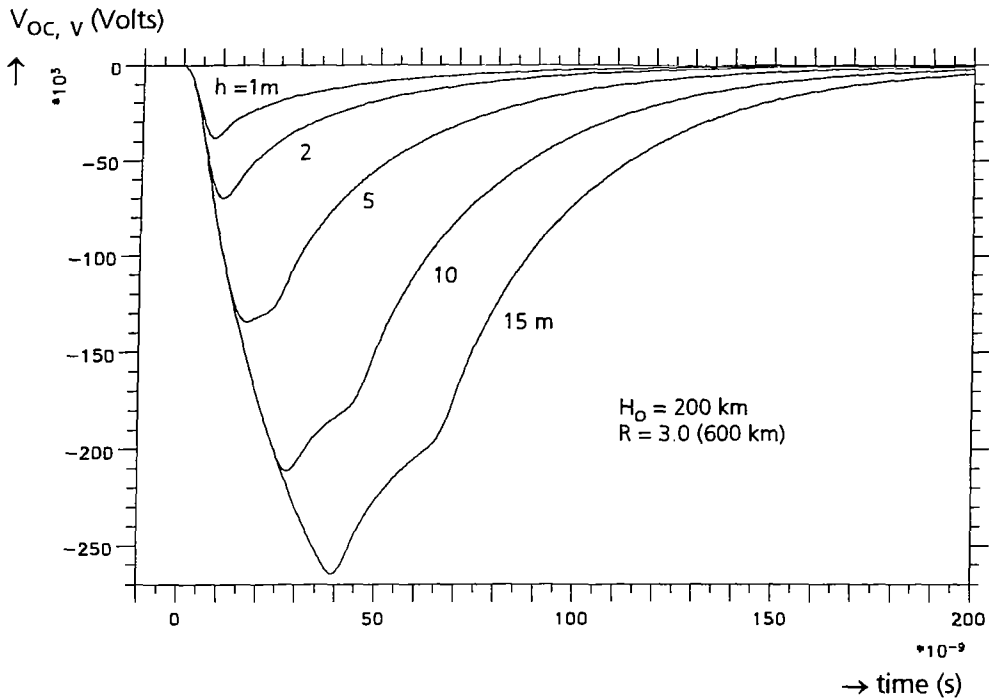
Because of the idealization of the problem (perfectly conducting ground, application of transmission line theory, neglectation of radiative losses) the oscillation remains undamped. A more rigorous treatment will be required for more realistic solutions.



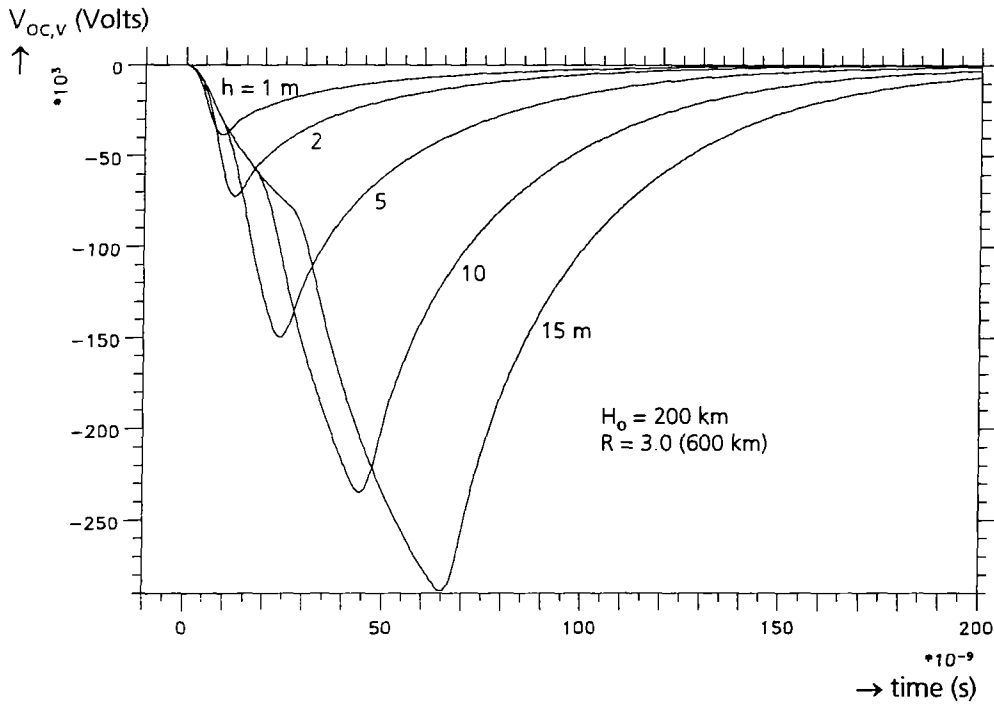
**Figure 22a**  
*Open-circuit voltages at base of a vertical element terminated at top in its characteristic impedance at various positions  $R$  (in units of  $H_0 = 200$  km) east of GZ ( $\phi = 0^\circ$ )*



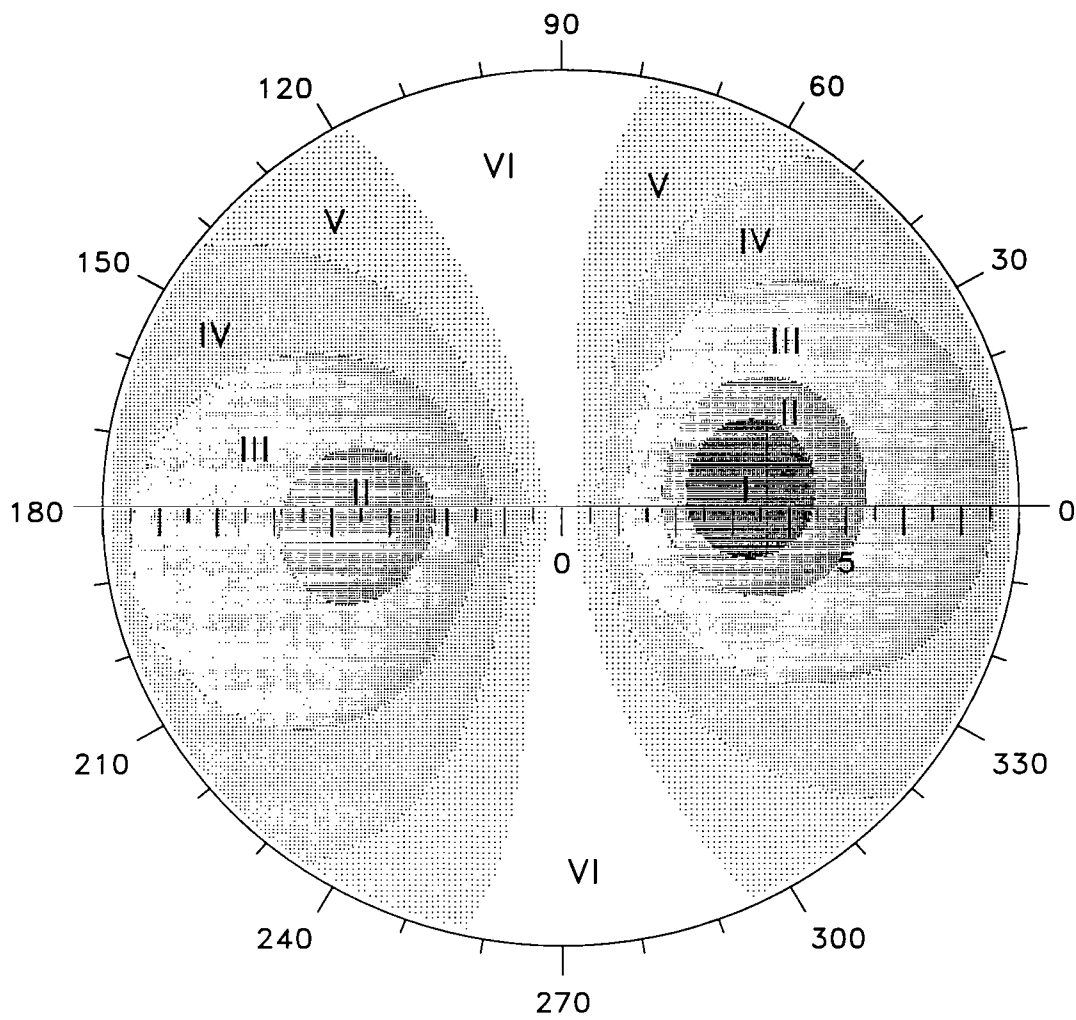
**Figure 22b**  
*Open-circuit voltages at top of a vertical element terminated at base in its characteristic impedance (i.e. no current reflections from ground) at various positions  $R$  (in terms of  $H_0 = 200$  km) east of GZ ( $\phi = 0^\circ$ )*



**Figure 23a**  
*Open-circuit voltages at base of vertical elements of various heights  $h$  terminated at top in their characteristic impedances at  $R = 600$  km east of GZ ( $\phi = 0^\circ$ )*



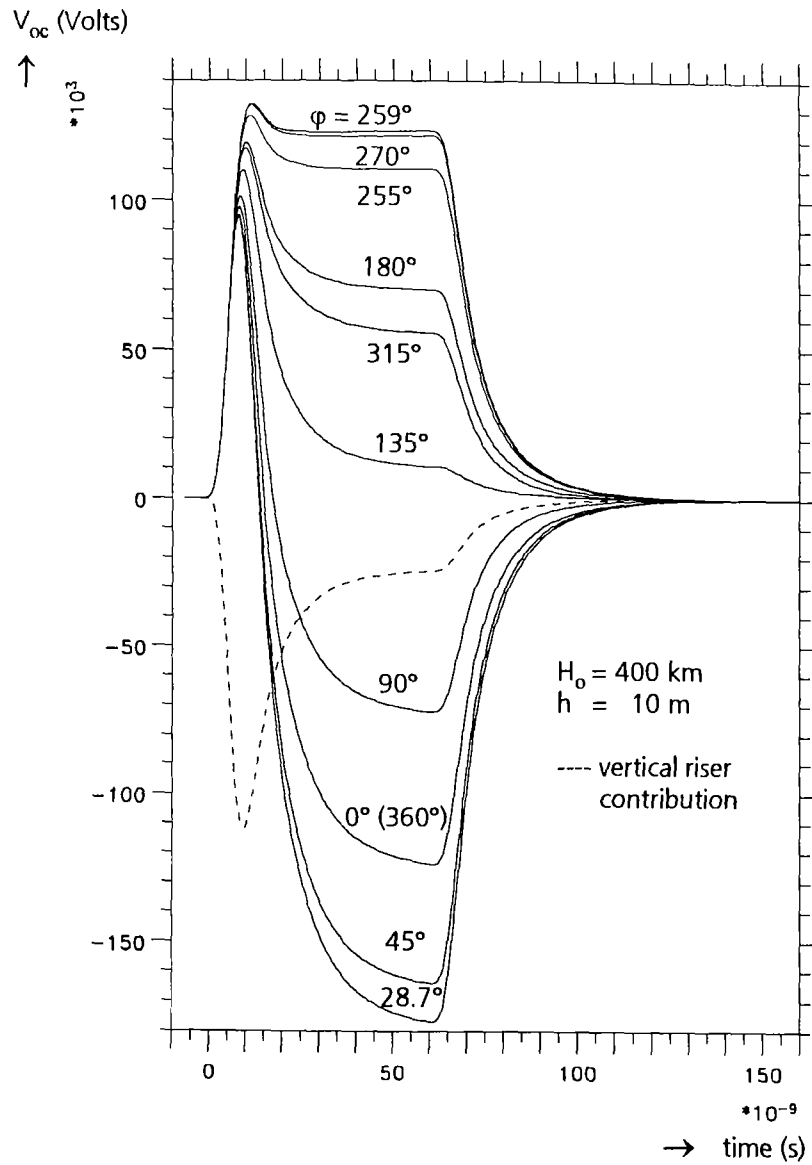
**Figure 23b**  
*Open-circuit voltages at top of vertical elements of various heights  $h$  terminated at base in their characteristic impedances (i.e. no current reflections from ground,  $\rho_0 = 0$ ) at  $R = 600$  km east of GZ ( $\phi = 0^\circ$ )*



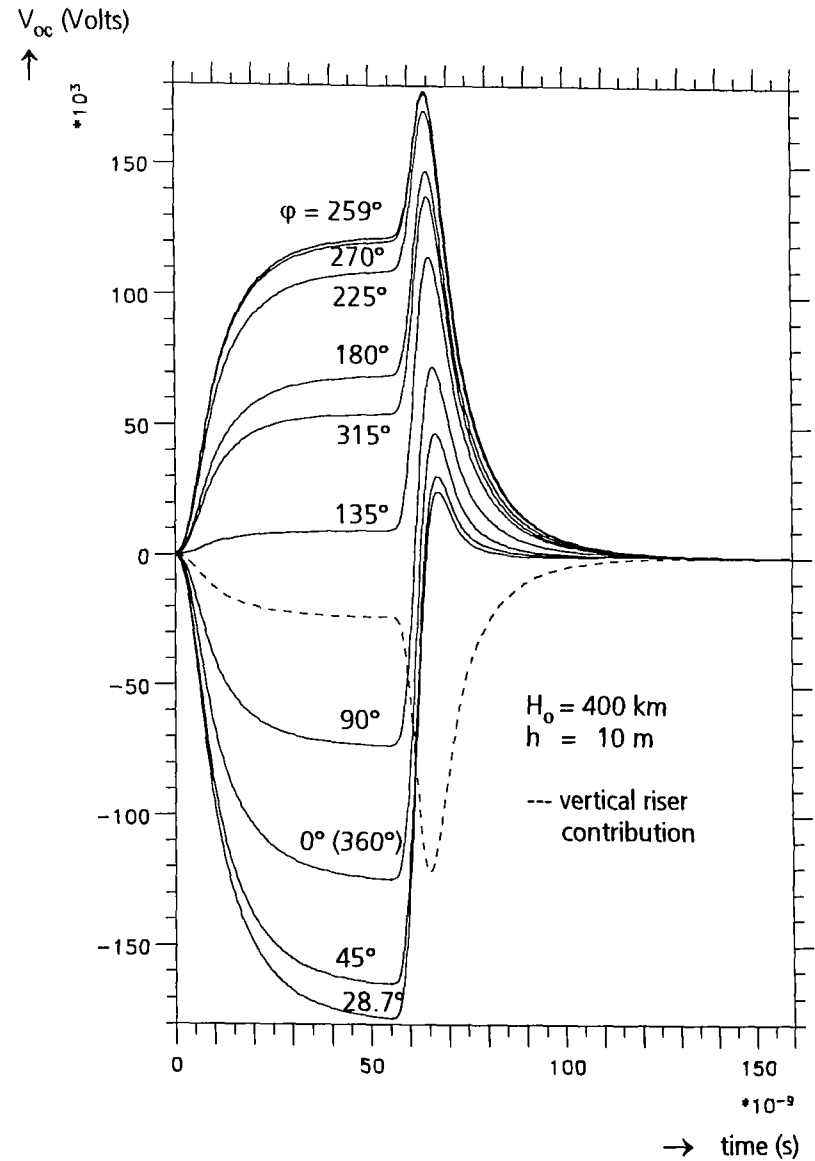
**Figure 24**

***Contour plot of the peak open-circuit voltages induced in a vertical element as calculated for case (IV)***

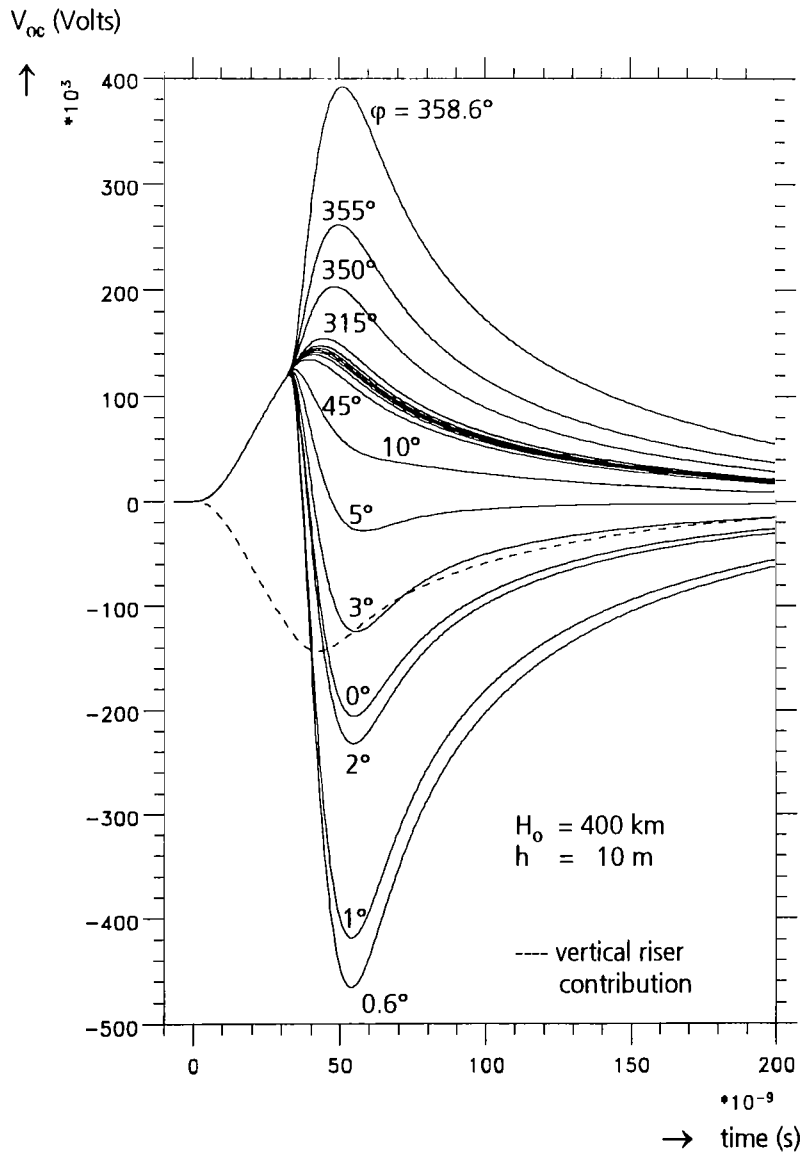
- I: 220 - 235 kV
- II: 200 - 220 kV
- III: 150 - 200 kV
- IV: 100 - 150 kV
- V: 50 - 100 kV
- VI: 0 - 50 kV



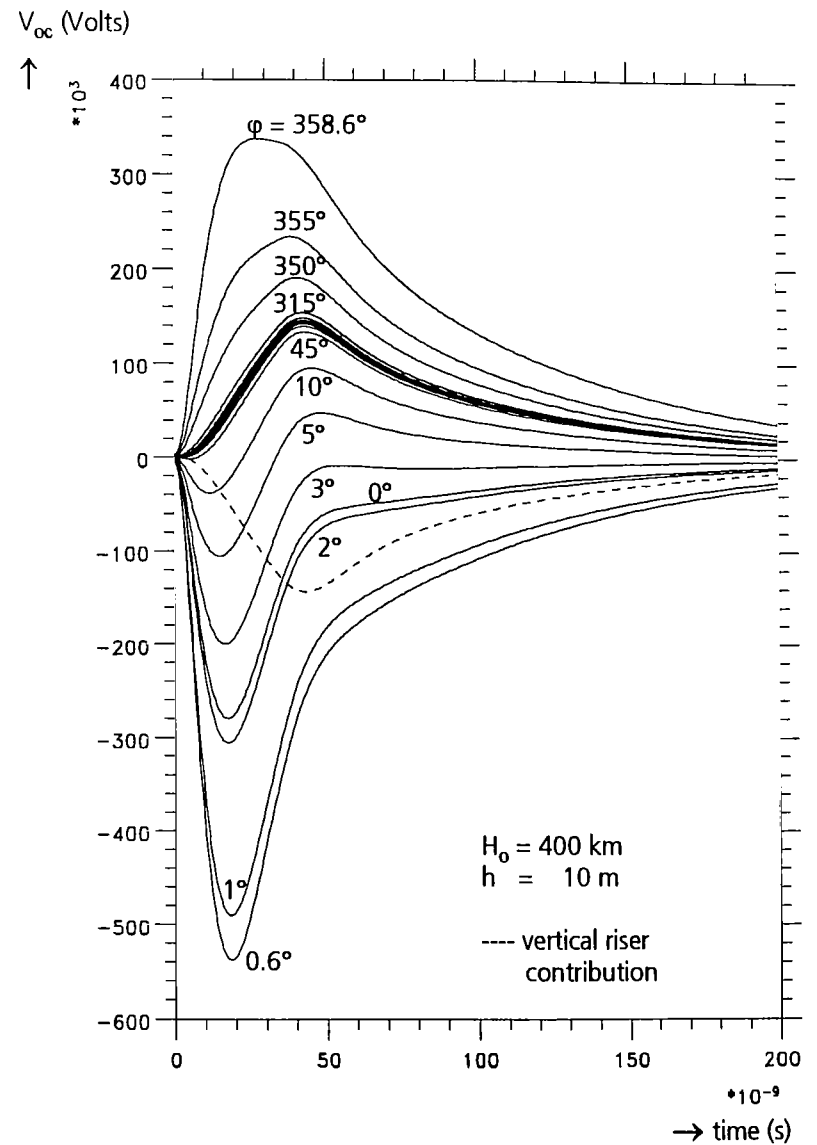
**Figure 25a**  
*Open-circuit voltages at the base of a vertical element connected to a semi-infinite horizontal line at  $R = 233.5 \text{ km}$ ,  $\phi = 0^\circ$ .*



**Figure 25b**  
*Open-circuit voltages between the end of a semi-infinite horizontal line and a vertical element terminated at ground by its characteristic impedance at  $R = 233.5 \text{ km}$ ,  $\phi = 0^\circ$ .*

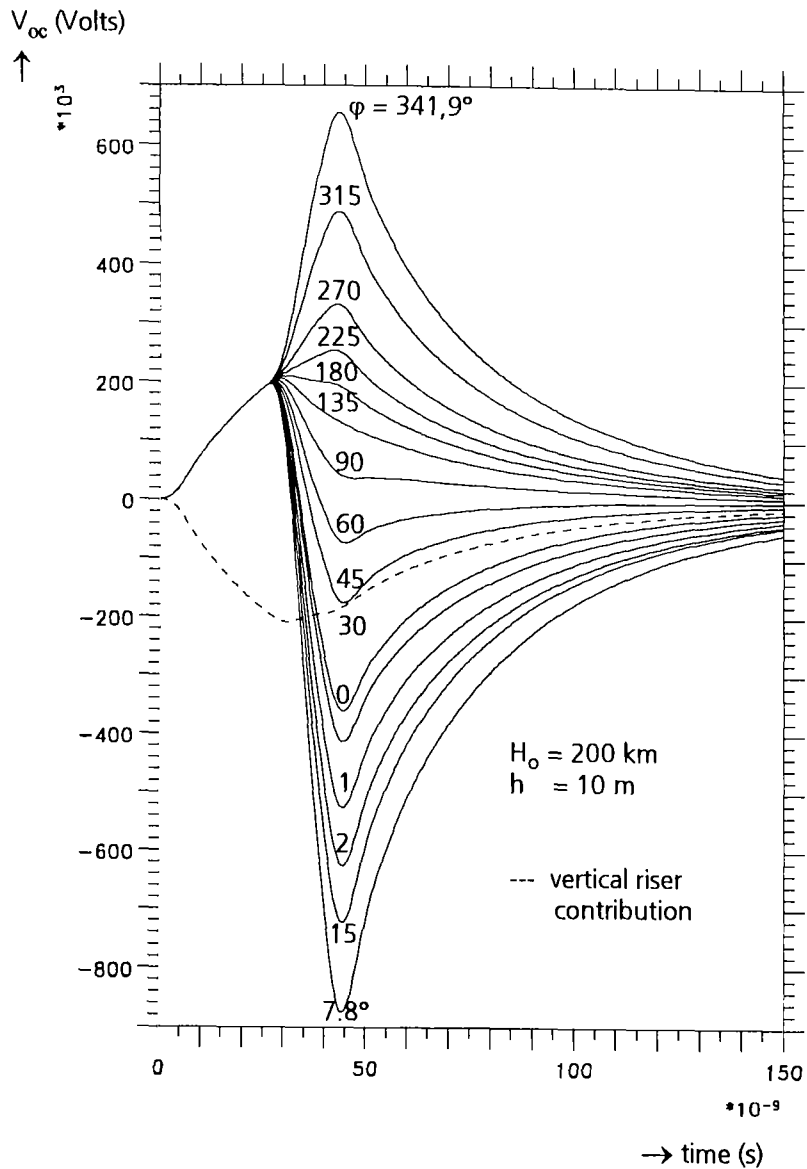


**Figure 26a**  
 Open-circuit voltages at the base of a vertical element connected to a semi-infinite horizontal line near the eastern horizon ( $R = 2100$  km,  $\phi = 0^\circ$ )

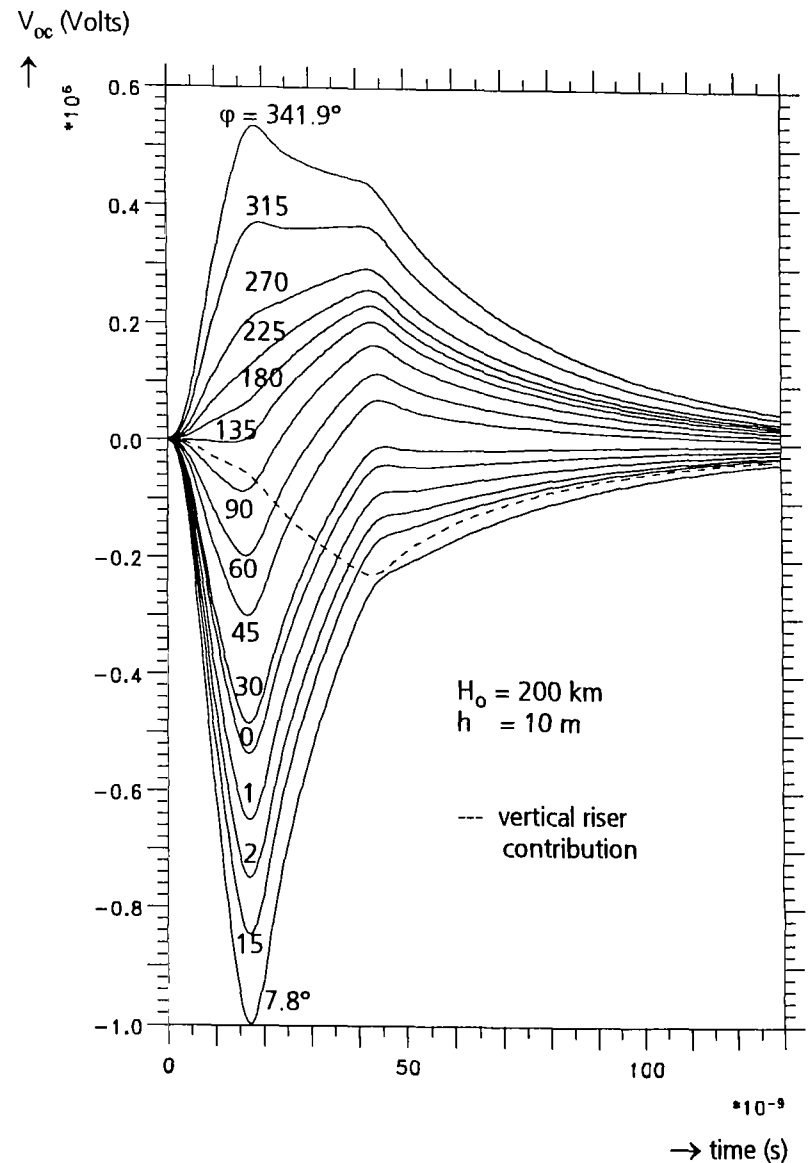


**Figure 26b**  
 Open-circuit voltages between the end of a semi-infinite horizontal line and a vertical element terminated at ground by its characteristic impedance near the eastern horizon ( $R = 2100$  km,  $\phi = 0^\circ$ )

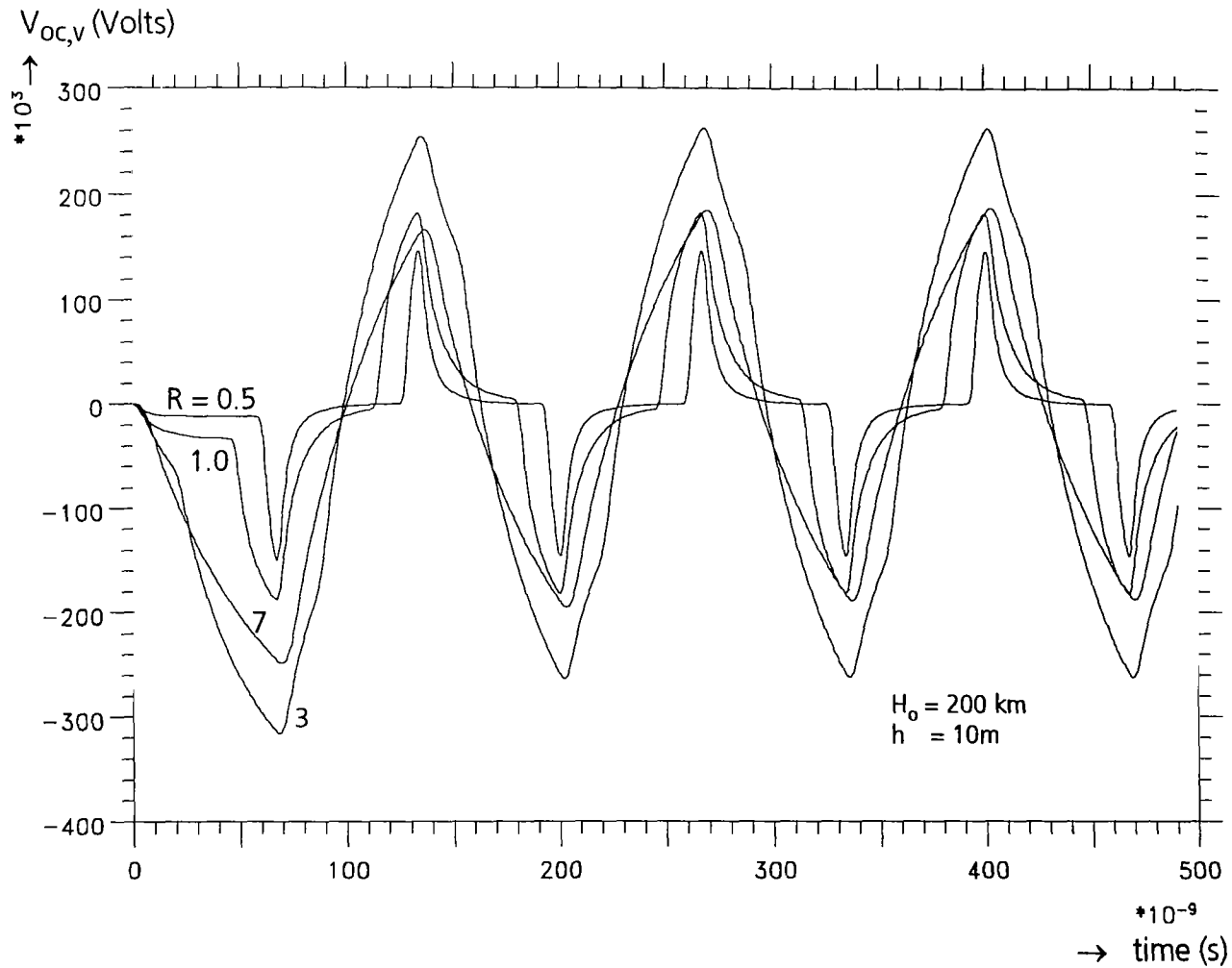




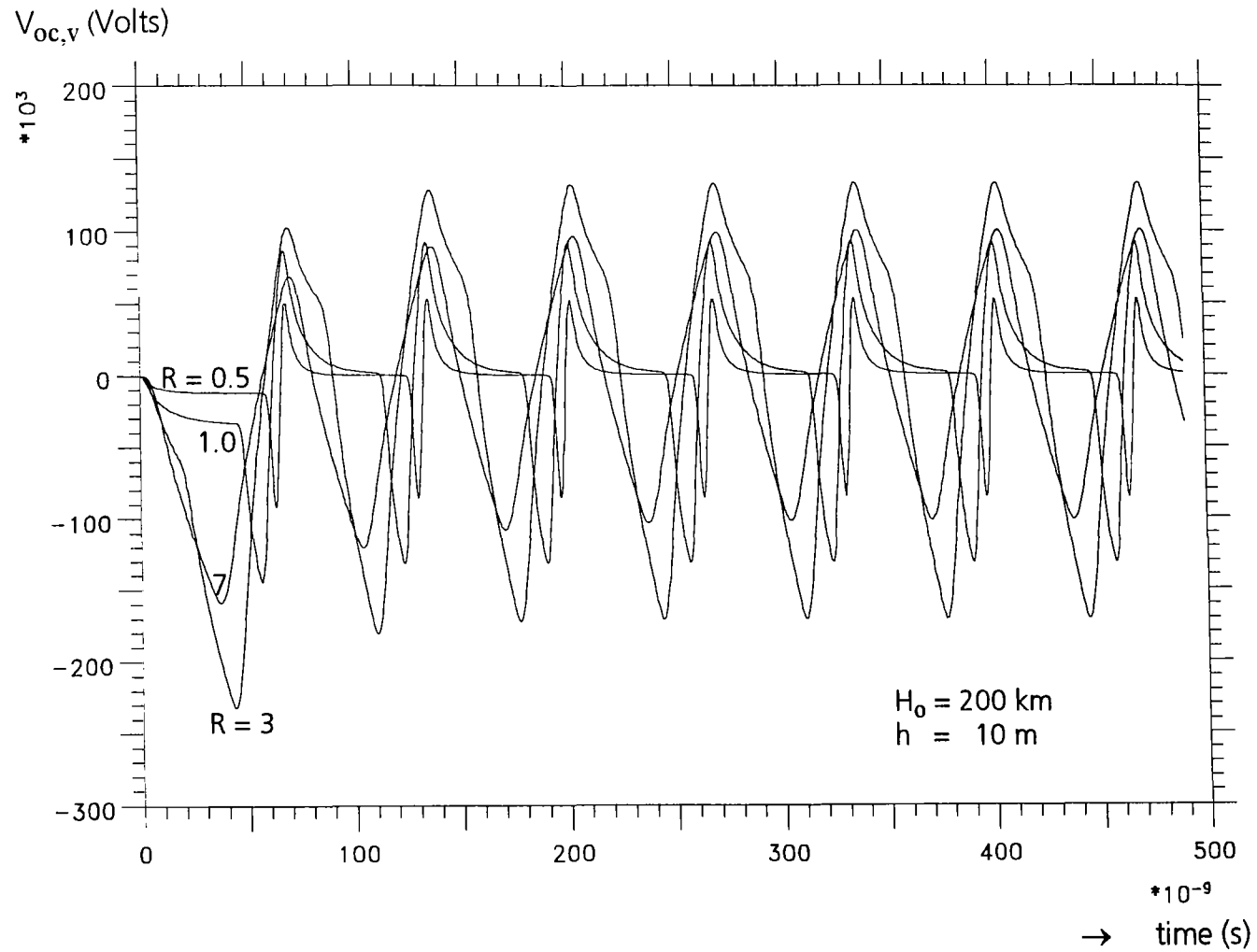
**Figure 27a**  
 Open-circuit voltages at the base of a vertical element connected to a semi-infinite horizontal line at the location of maximum response ( $R = 3.64 \times H_0 = 725$  km,  $\phi = -6.7^\circ$ )



**Figure 27 b**  
 Open-circuit voltages between the end of a semi-infinite horizontal line and a vertical element terminated at ground by its characteristic impedance at the location of maximum response.



**Figure 28**  
**Open-circuit voltages at top of vertical elements terminated at base in a perfectly conducting ground (reflection coefficient  $\rho_o = -1$ ) at various positions  $R$  (in units of  $H_0 = 200$  km) east of GZ ( $\phi=0^\circ$ )**



**Figure 29**  
*Open-circuit voltages at top of vertical elements not connected to ground (reflection coefficient  $\rho_O = 1$ ) at various positions  $R$  (in units of  $H_0 = 200 \text{ km}$ ) east of GZ ( $\phi = 0^\circ$ )*

## References

1. EMP Engineering and Design Principles, Bell Laboratories Publications, Whippany, NJ, 1975
2. Immunity to High Altitude Nuclear Electromagnetic Pulse - Description of HEMP Environment-Radiated Disturbance, IEC SC 77C (Sec) 20, 1994
3. F.M. Tesche, A Study of Overhead Line Responses to High Altitude Electromagnetic Pulse Environments, AFWL EMP Interaction Note IN 435, Kirtland AFB, December 1986
4. F.M. Tesche and P.R. Barnes, Development of a New High Altitude Electromagnetic Pulse (HEMP) Environment and Resulting Overhead Line Responses, Electromagnetics Vol. 8, p. 213, 1988
5. F.M. Tesche and P.R. Barnes, Transient Response of a Distribution Circuit Recloser and Control Unit to a High-Altitude Electromagnetic Pulse (HEMP) and Lightning, IEEE Transactions on Electromagnetic Compatibility, Vol. 32, No. 2, May 1990
6. C.L. Longmire, A Nominal Set of High-Altitude EMP Environments ORNL/Sub786-18417/1, 1987 and Theoretical Note TN 354 (1987)
7. K.-D. Leuthäuser, A Complete EMP Environment Generated by High-Altitude Nuclear Bursts, Theoretical Note TN 363, Phillips Laboratory, Kirtland AFB, 1992
8. K.-D. Leuthäuser, HEMP Environment: Data and Standardization, Theoretical Note TN 364, Phillips Laboratory, Kirtland AFB, 1994
9. K.-D. Leuthäuser, Distribution Functions of the HEMP Environment, Theoretical Note TN 365, Phillips Laboratory, Kirtland AFB, 1995
10. E.F. Vance, *Coupling to Shielded Cables*, Wiley Interscience, New York, 1978
11. W. Graf, HEMP Coupling into Lossless Wires over a Metal Surface (in German), INT Report No. 127, Euskirchen, Germany, 1987